University of Alberta

Gas Separation Membranes Using Cementitious-Zeolite Composite

by

Amir Hossein Shafie

A thesis submitted to the Faculty of Graduate Studies and Research

in partial fulfillment of the requirements for the degree of

Master of Science

in

Chemical Engineering

Department of Chemical and Materials Engineering

Spring 2012

Edmonton, Alberta

Abstract

Natural zeolite-based membranes have recently shown promise in the separation of H_2 from CO_2 and hydrocarbons. However, these highly dense, naturally monolithic materials can suffer defects which disrupt the continuity of the zeolite micropores and create leak paths through the membrane. Cement materials were explored as a component to generate mixed-matrix zeolite membranes. The ability for cement to intergrow between the zeolite particles promised to, under proper conditions, provide a smooth non-boundary interface with the zeolite particles and eliminate interparticle voids. The influence of zeolite contents in the composite membranes, operating pressures and temperatures on the performance of the membranes were examined. Gas permeation results show a hydrogen permeance of 4.1×10^{-8} $mol.m^{-2}.s^{-1}.Pa^{-1}$ a CO_2 permeance of 1.6×10^{-9} $mol.m^{-2}.s^{-1}.Pa^{-1}$ and a H_2/CO_2 single gas selectivity of 25 were obtained at 25^oC and 1 atm. The gas permeance through the clinoptilolite cement composite membrane was dependent on operating temperature, indicating that the permeation through the membrane was an activated diffusion process and that the permeation through the zeolite embedded in the composite membrane was predominant. However, the increase of gas permeation and the corresponding decrease of H_2/CO_2 selectivity with increasing total pressure are an indication of some defects in the composite membranes. Further research to optimize the membrane preparation conditions and to modify the membrane surface to improve hydrogen permeation and H_2/CO_2 selectivity is needed.

Acknowledgment

I would like to give my best appreciation to my supervisor Professor Steven M. Kuznicki for his priceless insight, patience and guidance on this project. I am also entirely grateful of my coworkers and technical lab staff because of their help. I want to thank Weizhu An for her help, critics, discussions, and conversations from time to time. Also I would like to give my best wishes to all my peer graduate students who made a friendly and p[productive environment during my research period, Omar Zarro, Paul Swenson, Brendan Tanchuk, Alireza Hejazi.

Finally, I give my best gratitude to my family and friends for the support they provided me during my graduate studies.

Table of Contents

List of Tables

List of Figures

Symbols	Description	Unit
α	Ideal selectivity	Unit less
d	Crystal plane distance	nm
λ	The wavelength of X-ray radiation	nm
ϕ	Concentration	mole / m^3
θ	Half of the diffraction angle	Radian
D	Diffusion coefficient	
ΔP	Trans membrane pressure difference	Pa
$P_{i,p}$	Partial pressure of component in permeate	Pa
$P_{i,f}$	Partial pressure of component in feed	Pa
$F_{i,}$	Molar flux of component i	mole / m^2 seconds
x	Diffusion length	m

List of Acronyms

CVD	Chemical vapor deposition
EDX	Energy dispersive X-ray analysis
GC	Gas chromatograph
GE	General Electric
ICP-MS	Inductively coupled plasma mass spectrometry
ILW	Intermediate-level radioactive wastes
MMM	Mixed matrix membranes
PEMFC	Polymer electrolyte membrane fuel cell
PPM	Parts per million
PSA	Pressure swing adsorption
PTFE	Polytetrafluoroethylene
RIF	Radioisotope facility
SEM	Scanning electron microscopy
STDEV.P	Standard Deviation based on the entire population
TCD	Thermal conductivity detector
TEM	Track-etch membrane
TGA	Thermogravimetric analysis
XRD	X-ray diffraction

Chapter 1: Introduction

1.1. Principals and concepts

The increasing demand for energy and the environmental concerns about fossil fuels are the driving forces behind the search for cleaner and environmentally friendly fuels. Hydrogen is considered to be one of the best candidates for the so-called clean fuels because the only product of hydrogen combustion is water (Nenoff, Spontak, & Aberg, 2006). Hydrogen is currently produced as a high temperature mixture with CO_2 (syngas), hydrocarbons and other impurities (H_2S, CO etc.), therefore, production of pure hydrogen almost always involves separation of hydrogen from syngas and/or hydrocarbons (Seidel, 2007). This separation is responsible for a big portion of energy consumption during hydrogen production.

Two common methods to purify hydrogen are pressure swing adsorption (PSA) and cryogenic distillation. While PSA units can produce pure hydrogen by repeating the adsorption/desorption cycle they are limited by their recovery value comparing with other systems (Kothari, Buddhi, & Sawhney, 2008). Cryogenic distillation systems are also less desirable due to their intense energy demand. Membrane technology promises to be a less energy-consuming approach to hydrogen separation. Barbaa et al. conducted a detailed comparison between conventional hydrogen production in a steam reforming plant with and without using a membrane. The significance of using a membrane system for hydrogen production is especially pronounced when its potential to combine separation and production step together is taken into account Based on this study introducing a hydrogen purification membrane combined with CO_2 removal can increase the overall efficiency of the separation up to ten percent (Barbaa et al., 2008). Various materials can be used as membranes from palladium

suggested in Barbaa's study to polymer membranes. The latter ones; however, suffer from two major disadvantages, the vulnerability of polymers to feed impurities such as hydrogen sulfide and hydrocarbons and the inherent poor thermal stability of polymers which limits their application in high temperature hydrogen separations (Robeson, 1999).

In contrast, zeolite molecular sieve membranes possess higher thermal and chemical resistance compared to the polymeric membranes and well defined pores/channels of molecular size. Therefore, they offer an alternative to selectively separate molecules based on their shape/size differences and adsorption properties (Caro & Noack, 2008).

1.2 Zeolites

Zeolite is a term used to refer to a crystalline aluminosilicate with a three dimensional silica (AlO_2-SiO_2) framework. Arrangement of species in this framework forms an ordered series of channels and pores of the molecular dimensions. Zeolite channels can carry a negative charge alongside the framework as Al^{3+} replaces Si^{4+}. Presence of alumina, in classic zeolites, and various other atoms (e.g. Ti, V etc.) enables zeolite surface to adsorb other molecules and compounds in its framework. Adsorption behaviour of zeolite differentiates species based on molecular size i.e. size exclusion and chemical properties. This molecular scale separation is usually referred to as 'molecular sieve'(Breck, 1973) phenomenon. Zeolites owe their huge commercial success to this molecular characteristic. Electron neutrality of zeolites is preserved by cations sitting in the pores and cavities. Some of the loosely held cations can be exchanged, providing zeolites with an important property of cation exchange.(Bekkum, 2001) Since the first scientific discovery of zeolites in 1756 by Swedish mineralogist Axel Fredrik Cronstedt, 194 different zeolite frameworks have been classified (Guisnet & Gilson, 2002). Among them 48 are

naturally occurring and the rest are synthesized in laboratory without a natural counterpart(McCusker, Olson, & Baerlocher, 2007). Zeolites ability to dehydrate without a change in crystalline structure made them a perfect candidate to be utilized in solar thermal collectors (Sand, 1978).

1.2.1 Natural Occurrence

Zeolites can be formed in a number of geological settings: (a) saline alkaline lake (b) saline alkaline soils (c) deep-sea sediments (d) low-temperature open hydrologic systems, (e) burial diagenesis. The common feature in all these geological settings is the availability of silica (SiO_2) alumina (Al_2O_3) and a cation e.g. calcium or sodium. The geological conditions and the nature of the alumina-silicate source affect zeolite formation as well as its properties. In saline alkaline lakes, silicic vitric tuffs change to deposits of zeolite mostly because of high alkalinity. In saline alkaline soils zeolites are formed on the surface as sodium carbonate concentrates by high rate of evaporation. Zeolite formed in deep-sea by the alteration of glass-bearing sediments into carbonate rocks containing zeolite. Clinoptilolite is a good example of an abundant natural zeolite and can be found in deep-sea sediments at depths greater than 100 meters. In burial diagenesis, temperature is the dominant factor in zeolite formation. Clinoptilolite and mordenite occurred in this setting can be thought of as minerals formed under high geothermal heat (Hay, 1986). These dense crystalline zeolites withstand thermally harsh conditions without a significant change due to the long-time exposure to harsh environments. The majority of natural zeolite resources found around the world are in impure tuff-like deposits. Therefore natural zeolites are excluded from most industrial applications (Ackley & Rege, 2003). In the course of this study however, we found pure, dense natural zeolite deposits that demonstrate promising separation characteristics.

1.2.2. Laboratory synthesis

Zeolites can be synthesized in a laboratory through slow crystallization of silica-alumina precursors. New zeolite frameworks that have absolutely no natural occurrence can be made in laboratory; however it is very difficult to make the product comparable to a natural crystal from the size and dimension point of view.

Zeolite synthesis usually involves the evolution of a reaction mixture from an initially random state to one with microscopic order (nucleation sites) proceeding to a final state where crystals (ordered atoms in a framework) can be observed. This crystallization process can be explained with two extreme mechanisms: solution-mediated transport and solid-phase transformation. Solution-mediated transport happens when aluminate/silicate species diffuse from a liquid phase to the nucleation site for crystal growth. In this method, synthesis starts with a clear solution i.e. no hydrogel (solid phase) is involved. On the other hand when a reaction mixture is prepared by adding solid precursors and a hydrogel is formed before nucleation, synthesis is going through a solid-phase transformation. Generally it is believed that zeolite crystallization route is dependent on the source of silica, e.g. sodium silicate yields a solid-hydrogel transformation while colloidal silica, e.g. Ludox, favours a liquid-phase transport mechanism (Davis & Lobo, 1992).

It has been proven that adding crystals as seeds to a crystallizing system will increase crystallization rate. This enhancement can be a result of increased available surface area or the introduction of new nucleation sites (Robson, 2001). Usually the presence of a crystal phase in the reaction substance induces formation of the same crystal phase. Secondary nucleation is used to distinguish this phenomenon rather than primary nucleation, which is simply crystal growth in

absence of foreign particles (*Zeolites and catalysis Vol. 1*, 2010). To synthesize a zeolite membrane not only all the steps involved in the preparation of zeolite crystals must be followed, but a special arrangement for successful transition between zeolite and support should be prepared. A synthetic zeolite membrane is usually made with several crystallization steps accompanied by careful seeding. Zeolite crystallization, happening through separate nucleation sites usually leads to grain boundaries which are not desirable for gas separation applications. A weak interface between support and zeolite crystals is also another concern in making a synthetic zeolite membrane. To date there still remain major technical obstacles before the successful application of synthetic zeolite membranes for gas separation.

1.3. Thesis outline

Recently An et. al. reported selective hydrogen separations from light hydrocarbons and CO_2 using natural zeolite clinoptilolite membranes (An et al., 2011). This thesis is outlines as follows: Chapter 1 introduces the concept of zeolites, its natural occurrence and a summary of how zeolites are synthesized in laboratories. Chapter 2 is a review on membranes, what they are usually made of and applications of zeolite membrane as well as cementitious systems comprising of natural zeolites. In Chapter 3 experimental set-up and analytical techniques are described. All the results are given in chapter 4 including permeation tests and characterization/stability tests. Finally in chapter 5 a summary along with suggestions for future studies are presented.

Chapter 2: Zeolite Membrane and Natural Zeolite Application Review

2.1. Membrane technology

Membrane technology is one of the oldest techniques for separating particles ranging from bacteria to molecules. Membranes can be used in liquid, gas or liquid/gas systems. Usually membrane systems are dominated by colloidal/molecular forces rather than the gravitational force. Generally, membranes are selective barriers that can control permeation of species through their structure. First scientific uses of membranes date back to the eighteenth century (Cardew & Level, 1999). For a long time membranes were only used as laboratory tools to investigate other conceptual theories. Van't Hoff's use of osmotic pressure measurements made by Traube and Pfefferin (1887) to develop his famous equation is an outstanding example (Baker, 2007).

2.1.1. Membrane materials

Various materials have been tried in three basic designs for separation membranes (a) flat sheet, (b) hollow-fibre (c) tubular. The frequently used membrane structures are outlined below (Cardew & Level, 1999).

Dense films

This simple membrane structure is widely used for ion-exchange membranes and electrodialysis. Different techniques can be used to make a dense film of a polymer with cation/anion exchange ability. Chemical vapour deposition (CVD) (Park & Sudarshan, 2001) and plasma are among them. Dense film membranes are limited by complications in their preparation process (Adhikari & Fernando, 2006). In their use in fuel cell applications, dense film membranes went through a long history of turning points with introduction of new materials. Development of Nafion is an

example; crystalline regions of PTFE contribute to hold the membrane against swelling while hydrophilic groups provide a channel for water and charged species to pass through (Roualdes et al., 2007).

Homogenous microporous membranes

Stretched polypropylene are among the industrially manufactured membranes. They can be categorized as homogenous microporous materials (Sadeghi, Ajji, & Carreau, 2007). Stretching degree, particle/filler size and content are adjustable factors that have been studied (Mizutani, Nakamura, Kaneko, & Okamura, 1993). The membranes are mainly used in vapour/liquid separation due to their interesting hydrophobic/hydrophilic characteristics(Lawson & Lloyd, 1997). The second example of homogenous microporous membrane is track-etch polycarbonates (TEM). TEM has found applications in laboratory filtration, cell-related research and biosensors. TEM owe their useful surface properties to their controllable pore size/pore shape. Use of heavy ion accelerators in TEM preparation process makes it possible to design the etching characteristic for the desired application. However they are still limited for gas separations at elevated temperatures due to their polymeric nature (Apel, 2001).

Asymmetric membranes

Asymmetric is a general term referred to a membrane structure with different pore size in the feed and permeate side (Wienk et al., 1996). Solution phase inversion is the most common method to make an asymmetric membrane. The preparation process involves transformation of a homogenous solution into two, polymer rich and solvent rich phases. Two phases ultimately become the rigid and porous media for separation (Cardew & Level, 1999). Lee et al recently reviewed advances in this field of membrane science specifically regarding reverse osmosis (Lee, Arnot, & Mattia, 2011).

Ceramic membranes

Ceramic membranes were first manufactured to address separation needed in the nuclear industry i.e. uranium isotopes (Mendes, Magalhaes, & Costa, 2006). However, their ability to function in harsh chemical and thermal environments has led to their applications in other areas. Alumina, titania and zirconia are among the common materials made into ceramic membranes. Sometimes in the literature zeolite membranes are referred to as a subcategory to ceramic membranes, however ceramic membrane are more often used as supports to other types of separating agents (zeolites, metallic layers etc.) due to their larger pore size (Jia, Chen, Noble, & Falconer, 1994).

2.1.2. Zeolite membranes

As discussed earlier in Chapter 1 zeolite crystals can be synthesized using a hydrothermal crystallization process, which is normally nucleation of zeolite crystals in an alkaline solution in a moderate temperature/pressure system. (~80 ^{o}C/autogenous pressure). A popular approach to prepare zeolite membranes is to immerse a porous support in the zeolite synthesis solution, proceeding by controlled crystallization of a thin zeolite layer on the support (Caro & Noack, 2008). Alumina or stainless steel was chosen to serve as the support material.(Li et al., 2011). Synthesis of supported thin zeolite membranes for large-scale hydrogen separations, however, needs to overcome technical and material challenges such as a strict demand of support properties, tedious synthesis process and fatal defect formations due to the poor support-zeolite material property compatibility (Caro, Noack, Kölsch, & Schäfer, 2000).

Two recent cases of synthetic zeolite membranes will be discussed here as examples. Tin (Sn) and titanium zeolitic membranes were synthesized in a framework structure similar to umbite mineral (Sebastian et al., 2006). A porous α-alumina tube with a pore size of 1.900 μm was seeded with umbite particles simply by rubbing the seeds to the support. The tube then

contacted with a substrate gel which has fumed silica as its silica precursor. The main crystallization step was conducted at 230 ^{o}C for 48 hours. The result is a 5 cm long zeolite/α-alumina tube which was tested for permeation tests in the temperature range of 30 to 150 ^{o}C. The authors observed an increasing trend of permeation with temperature as an indication of activated diffusion. However testing gases had a different correlation with temperature. The reported value of H_2 permeation varied with different membranes as well as gas mixtures. The authors noticed the existence of intercrystalline defects by following gas permeation trends in different species.

In the second case, Li and coworkers successfully synthesized a zeolite framework structure with no natural occurrence (Li et al., 2011). A titano-silicate zeolite membrane (known as AM-3) was hydrothermally synthesized on a tubular α-alumina and a stainless steel support with an average pore size of 3 and 0.5 μm. Sodium silicate was the silica precursor while crystallization was conducted at 350 ^{o}C for 48 hours. It is emphasized that crystallization time dramatically decreased form 17 days to 48 hours by using proper seeding steps. Permeation studies were conducted on AM-3 supported membranes in the temperature range of 25 to 120 ^{o}C and activated diffusion for hydrogen was observed. Top view scanning electron micrographs however show gaps among zeolite crystals. This can easily jeopardize gas separation ability of the zeolite membrane because gas molecules instead of selectively diffusing through the zeolite crystals pass through intercrystalline gaps.

Another general approach to zeolite membrane preparation is the matrix composite also known as Mixed Matrix Membranes (MMM). The core idea is to combine or embed the separation reagent with or into a continuous matrix material. Thus, instead of the synthesis of a thin layer on the support, integrity of the membranes is provided by the matrix. It has been

reported that matrix membrane of zeolite nano/meso particles embedded in polymeric membranes showed improved thermal, mechanical strength and separation performance as compared to the pure polymeric membranes (Süer, Baç, & Yilmaz, 1994). However, these matrix membranes suffer from limited applications in high temperatures (above 200 ^{o}C) due to the inherent properties of the matrix polymer (Miller, Koros, & Vu, 2007). The efficient separation performance of MMM depends on the separation agent, chemical and physical compatibility of the matrix and the separation agent materials. (Zimmerman, Singh, & Koros, 1997).

2.2 Natural zeolite applications

The first users of natural zeolites were the Romans; they used mined rocks in buildings and constructions. However one of the earliest published studies on applications of natural zeolites in recent times is by Hafez et. al. who studied potential applications of natural zeolites in purification of low level radioactive wastewater (Cesium and strontium) (Hafez, 1978). A similar approach was used by Erdem and co-workers to study natural zeolite clinoptilolite, in order to assess its feasibility for cleaning metal industry wastewater. Clinoptilolite showed a strong affinity to adsorb heavy metal cations from aqueous solutions (Erdem, Karapinar, & Donat, 2004). In a very interesting study Ok studied a commercial adsorbent called Zeo-Ads which is prepared by a mixture of Portland cement and natural zeolite powder. Yong showed that this product can remove lead (Pb) and copper (Cu) from an aqueous solution (Ok, 2007). Portland-zeolite adsorbent prepared by mixing of two powders with a weight ratio of Portland to zeolite of 1:3 in a vacuum extruder, aging in water for 30 days and finally baking in a furnace at 400 ^{o}C for 3 hours.

In two separate studies clinoptilolite and chabazite were used to crack heavy bitumen from Canadian oil sand industries (Kuznicki et al., 2007). in these studies natural zeolite performed as

catalyst cracking high molecular weight organic compounds to value-added processable products.

2.3 Natural zeolite/cementitious systems

Portland cement and its various applications have been known for decades. Portland cement is made by heating a mixture of limestone and clay up to a degree where partial fusion occurs, about 1450 ^{o}C. The product may contain 67 % calcium oxide (CaO), 22% silicon dioxide (SiO_2), 5% aluminum oxide (Al_2O_3) and 6 % of other components (Hewlett, 2008). Cement in its dry powder form is a multi-phase inorganic material with four major phases called alite, belite, aluminate and ferrite. Cement hardening results from reactions between the major phases and water.(Taylor, 1990) Cement and concrete have their own nomenclature[1] The hydration reaction can be represented by the following three equations.(Hewlett, 2008)

$$C_3S + H_2O = C\text{-}S\text{-}H + nCH \text{ (calcium hydroxide)} \qquad (2.1)$$

$$C_3A + 3C\underline{S}H_2 + 26H = C_3A \,.\, 3C\underline{S}H_{32} \text{ (ettringite)} \qquad (2.1)$$

$$C_3A \,.3C\underline{S}H_{32} + 2C_3A + 4H = 3C_3A \,.\, C\underline{S}H_{12} \text{ (monosulphate)} \quad (2.3)$$

Cement is produced around the world in huge quantities every year. A large majority of that is being used in general construction applications. The standard specifications to evaluate cement are generally based on its chemical composition or physical property. Standard performance tests have also been designed such as setting time or compressive strength (Bye, 1999).

[1] C : CaO, A : Al_2O_3, S : SiO_2, $\underline{S}$: SO_3, H : H_2O

Various types of cement are produced that differ in hardening time, sulfate and thermal resistance and physical appearance among others. White Portland cement for example, can be made by increasing the ratio of Al_2O_3 to Fe_2O_3. Type II cement is defined by ASTM[2] C150 as a moderate heat hydration cement. Composite cement is used when one or more inorganic materials are added to cement for the purpose of making a substantial change in hydration reaction and its products. In a study done by Janotka and co-workers (Janotka, 2003) zeolite blended Portland cement was tested for resistance to acidic and sulfate attack. The experiment showed an increase in both acid and sulfate resistance, which can be explained by the availability of a larger surface area for reaction resulting in stronger structure. Natural zeolite contribution in hydration reaction may decrease the amount of harmful large pores due to zeolite's microstructure.

Perraki et al conducted a Chapelle test on a natural zeolite sample (heulandite) in order to measure the activity of natural zeolite to participate in a hydration reaction. Chapelle is a standard test involving zeolite reaction with calcium hydroxide, $Ca(OH)_2$, in a boiling aqueous solution for 16 hours. Calcium hydroxide consumption after the test indicates the zeolite pozzolanic activity that is defined as the ability of a material to form cementitious matrix. According to Chapelle 0.555 g of calcium hydroxide were consumed per gram of zeolite which is higher than reported value for flyash, 0.360 g/g flyash[3] (Adamiec, Benezet, & Benhassaine, 2008) (Perraki, Kakali, & Kontoleon, 2003). Ortega in a study with clinoptilolite in alkali activated systems reported a significant amount of unreacted zeolite even after long hydration times (Ortega, Cheeseman, Knight, & Loizidou, 2000).

[2] American Society for Testing and Materials

[3] Flyash is fine silica based particles rises with flue gas in combustion furnaces. Recently it has been researched to be used as a cement/concrete supplement.

Ahmadi and Shekarchi in a more recent work studied the use of natural zeolites as a supplementary material to cement (Ahmadi & Shekarchi, 2010). They measured oxygen gas permeability as well as various physical and durability tests. They reported a decrease in gas permeation compared to a concrete sample without zeolite, followed by a jump in permeation as the amount of zeolite increased. The authors related this behavior to the extra unreacted zeolite in the matrix and its contribution to the gas transport.

Cement paste has also been investigated for its gas permeation characteristics. Frizon at The Atomic Energy Commission of France reported diffusive transport of hydrogen through a hardened cement paste. This report which was aimed to investigate the long-term management of intermediate-level radioactive wastes (ILWs) showed a direct relation between hydrogen permeability and the degree of cement hydration, i.e. as the hydration increases the hydrogen flux drops significantly (Frizon & Galle, 2009). As far as concrete and gas permeation is concerned it is worth to mention the work by Daoud and Renken (Daoud & Renken, 2001). They used standard construction concrete common in Wisconsin area in combination with a commercial polymer membrane as a retardant to radon gas diffusion. They successfully reported a system of polymer-concrete with more than 98% gas penetration reduction.

In another composite cement study conducted by Shen alumina cement was added to a graphite[4] membrane used for polymer electrolyte membrane fuel cell (PEMFC) (Shen, 2006). Mould and press was used to prepare samples of 5mm width, and 2.5mm thickness followed by 7 days moisture treatment in an environment with 100% relative humidity. With the aforementioned procedure the authors could achieve the desired flexural strength due to intergrown and mutual penetration of cement hydration products.

[4] Poco ^{TM} graphite membrane commonly used accounts for 60% of the cost

Use of autoclave in cement preparation was studied by Lehmann and coworkers (Lehmann, 2009). In this work evolution of different phases were investigated during and after hydrothermal treatment at 200 ^{o}C. The autoclave step initiates a transformation in the cement microstructure. These series of reactions leads to a more homogeneous structure with “healed” flaws.

In this study application of zeolite-based cementitious membrane for gas separation was investigated in order to improve manufacturability of dense natural zeolite membrane. Successful application of this idea may avoid disadvantages attributed to zeolite membrane preparation discussed earlier.

Chapter 3: Experiment and Procedure

3.1. Experimental apparatus and materials

As reviewed in the second chapter, zeolite membranes can be utilized as an excellent potential medium to separate gaseous species. In spite of significant developments synthetic zeolite membrane technology is not yet mature enough for commercial use. The main focus of the experimental part of this project is to adopt a novel approach in order to utilize zeolite membranes while avoiding major drawbacks associated with synthetic membranes like tedious and time-consuming preparation, inevitable cracks due to thermal expansion and potential inter-crystalline gaps. This chapter addresses:

a) Overall understanding of the materials used in the project.

b) Material characterization using sophisticated methods common in this field.

c) Methodology used to prepare samples.

d) Description of the test procedure.

The next chapter shall provide the test results along with detailed characterization assessments of materials used in the project.

3.1.1. Materials

Two different natural zeolites used in this work are clinoptilolite and mordenite. Stock samples were obtained directly from two mining companies (Blue Pacific Minerals New Zealand, Badger Mining Company LLC - Amargosa Valley Nevada) Original samples were bulky rocks rich with clinoptilolite/mordenite mineral.

Clinoptilolite has a complex formula of $(Na,K,Ca)_{2\text{-}3}Al_3(Al,Si)_2\ Si_{13}O_{36}\cdot 12(H_2O)$. It has the same framework structure as heulandite determined by Merkle and Slaughter in 1968 and the term 'isostructural' is commonly used to refer to these minerals (Sand, 1978). Clinoptilolite samples from different deposits are tested. In some cases traces of heulandite were observed. These two minerals are recognisable in terms of Si/Al ratio and cation content. As Si/Al ratio determines most properties of zeolites, a distinct behaviour was expected. Silicone/Aluminum ratio can vary from 2.7 in heulandite to 5.3 in clinoptilolite. This chemical property of clinoptilolite makes it more important than its isostructural mineral twin from stability[5] point of view (Sand, 1978).

Clinoptilolite has a 2-D channel system including two channels running parallel to each other and a third channel intersecting the two channels (eight member ring) in a perpendicular angle, Figure. 3.1. letters A and B corresponds to eight and ten member ring parallel channels respectively (Bonneviot & Kaliaguine, 1995).

[5] Stability refers to the ability of zeolite to have its desired functionality while exposed to operating environment

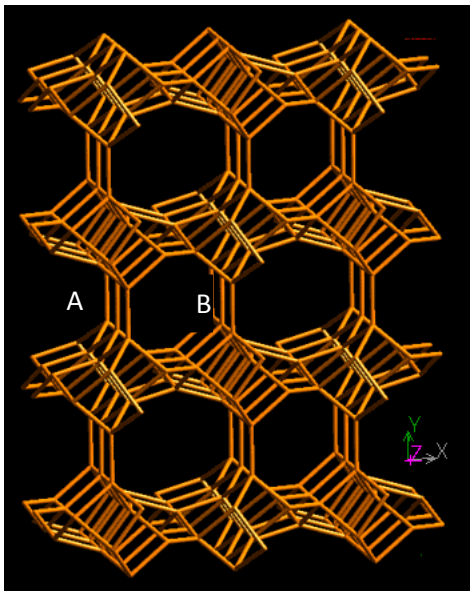

Figure 3.1 Clinoptilolite framework structure, Viewed along [001].Picture from Structure Commission of the International Zeolite Association

Mordenite on the other hand has a different framework structure with a chemical formula of (Ca, Na_2,K_2)$Al_2Si_{10}O_{24}$·$7H_2O$) (Sand, 1978). As zeolite structures have been classified on the basis of secondary building unit, mordenite is classified as 12-member ring zeolite (Figure 3.2) (Korkuna et al., 2006).

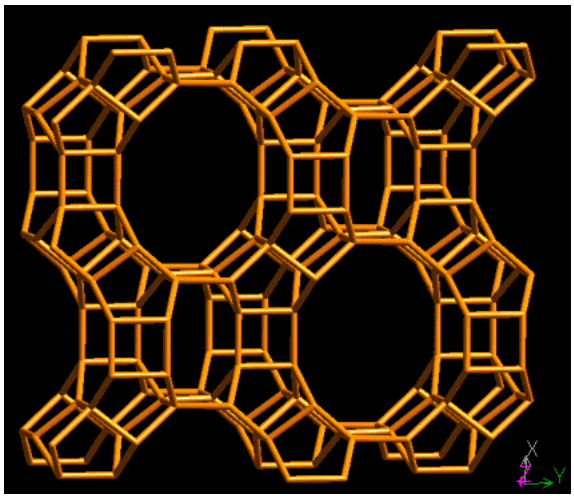

Figure 3.2 Mordenite framework structure, Viewed along [001].Picture from Structure Commission of the International Zeolite Association

Mordenite crystals can be found in nature in altered volcanic deposits. It has a higher Si/Al ratio than most other natural zeolites which makes it more stable in harsh chemical and thermal environments. Due to its thermal stability of mordenite has been used as catalyst in various reactions (Aguado, 2009). Various studies have reported improvements in catalytic properties of mordenite by different chemical and physical methods (Paixão, 2010).

3.1.2. Raw membrane preparation

Zeolite samples were obtained in ‘as mined’ form. These bulks of rocks were sectioned by a diamond saw into discs approximately 1.25 cm in diameter. A rotating polisher equipped with a diamond lapidary disc was used to polish discs down to 1.0 - 1.5 mm thick, followed by washing with deionised water. Clean discs were dried in an oven at 120 °C for at least 2 h. before further pre-treatments and mounted in the testing apparatus. In this work these samples are referred to as ‘raw’ membranes.

3.1.3. Cementitious composite membrane preparation

Dry clinoptilolite powder (mesh size 325 ~ 44 μm) were well mixed with Portland cement in an alumina mortar and pestle. The weight ratio of zeolite to cement was varied in the range of 2:1 to 7:1(zeolite: matrix). This mixture was made into a disc using a uniaxial hydraulic press. Initial mass of dry powder packed into the ¾” diameter die was controlled to get the desired membrane thickness. The maximum pressure limit was 22 tons per square inch which was kept constant to calibrate membrane thickness with the mass of powder to be packed. After pressing, the membrane discs were cured by steam in a 500 mL Teflon lined stainless steel autoclave overnight (approximately 15 hours). Steam temperatures were varied from 120~250^{o}C to find the optimal curing conditions. Before gas permeation tests all matrix membrane samples were dried at 300^{o}C in a temperature programmable muffle furnace in ambient atmosphere. The temperature controller of the furnace was set to ramp at 1^{o}C/min from room temperature to 300^{o}C and kept at 300^{o}C overnight. Figure 3.3a shows a stepwise process of composite membrane preparation. Figure 3.3b illustrates a rock sample, a raw and a composite membrane.

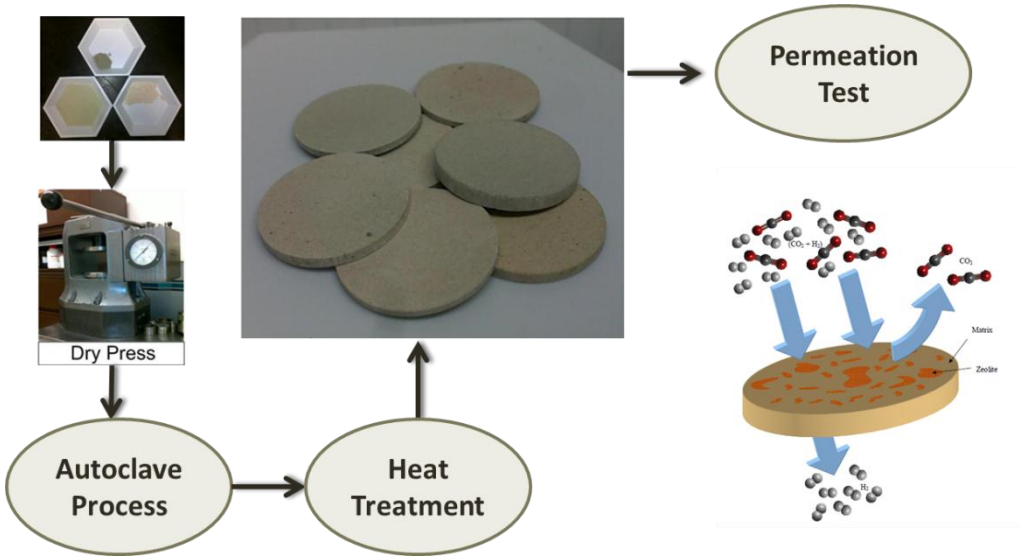

(a)

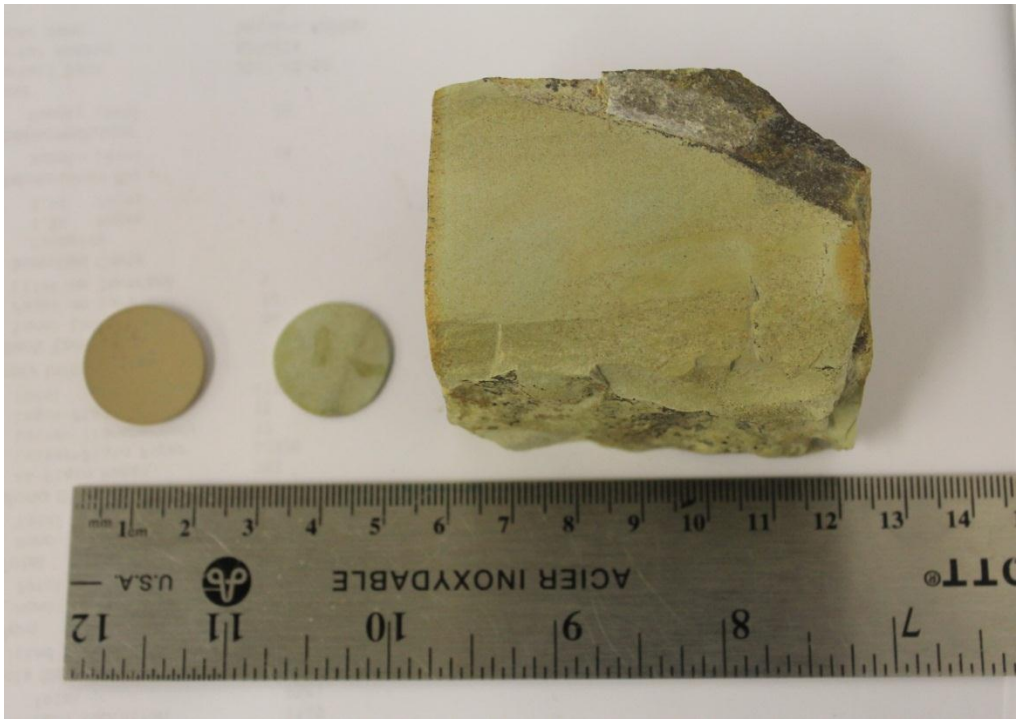

(b)

Figure 3.3a (Left to right) Stepwise process of composite membrane preparation

Figure 3.3b (left to right) A mordenite composite membrane, a raw mordenite disk and a rock sample

3.1.4. Permeation test apparatus

Gas permeation through the zeolite cement matrix membranes were measured using a stainless steel membrane testing system shown in Figure 3.4. The membrane was sealed in a stainless flanged cell between two graphite gaskets. The feed and permeate sides of testing chamber were separated by the membrane. Each side of testing chamber attached to a stainless steel tube (OD=1/2") where feed and sweeping gases (Ar) entering through tube sides, while permeate and retentate leaving through the shell sides. The flanged membrane cell was placed into a tube furnace with a multipoint programmed temperature controller. For permeation tests at higher temperatures a heating rate of 5 ^{o}C/min was used between runs before steady state condition was reached. Permeation tests were conducted in constant isothermal temperatures. Transmembrane pressure was controlled by a back pressure regulator located at the feed side outlet. The feed and sweeping gas flowrates were controlled by two mass flow controllers (Sierra Instrument Inc.). The flowrates of the feed and sweeping gas were constant at 100 mL/min (STP) and 200 ml/min (STP) respectively, for all gas permeation tests. The flow rate of outlet streams was measured using bubble flowmeters (Figure 3.5 and 3.6)

An on-line GC (Shimadzu Gas Chromatograph GC-14B) equipped with a TCD and a packed column (HaySep Q, 80~100mesh) was used to analyze the outlet gas concentrations. Helium and Argon were used as GC carrier gases for CO2 and hydrogen analysis respectively.

The following equations were used to calculate permeance according to Fick's law of diffusion (Bird, Stewart, & Lightfoot, 1976).

$$F_i = -D \frac{\partial \emptyset}{\partial x} \qquad (3.1)$$

Where F_i is amount of substance in per unit are per unit time ($\frac{mol}{s.m^2}$), ϕ for ideal mixtures is concentration (in this case is represented by pressure) and D is diffusion coefficient in dimensions of $\frac{m^2}{s}$. With substation of pressure for concentration equation (3.1) changes to:

$$F_{i} = -D \frac{\Delta P}{\Delta x} \quad (3.2)$$

Where ΔP is transmembrane pressure difference and D is defined in $\frac{mol}{s.Pa.m}$.

$$\Delta P_i = (P_{i,f} - P_{i,p}) \quad (3.3)$$

Permeance is then defined in dimensions of $\frac{mol}{Pa.\,s.m^2}$:

$$\text{Permeance} = \frac{F_i}{\Delta P_i} \quad (3.5)$$

The testing gas assumed to follow ideal gas behaviour regarding working pressure and temperature.

Gas permeation set-up was tested with a standard Alumina membrane provided by General Electric (GE) gas membrane research group.

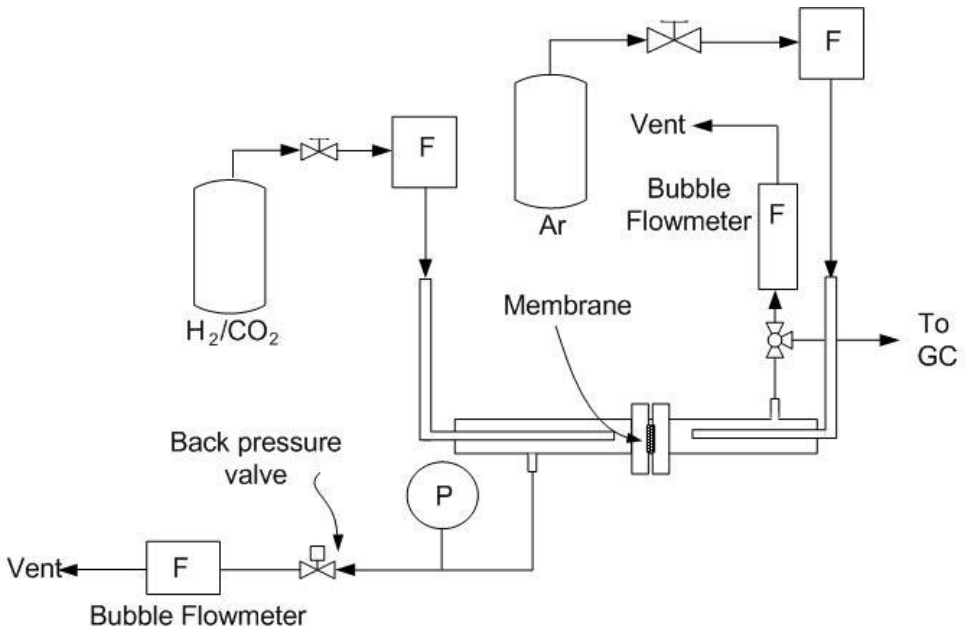

Figure 3.4 Schematic diagram of testing apparatus

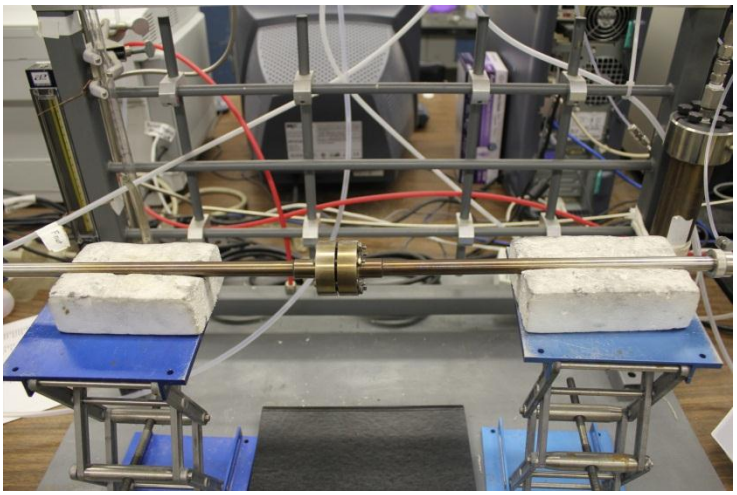

Figure 3.5 Flanged membrane chamber for permeation test

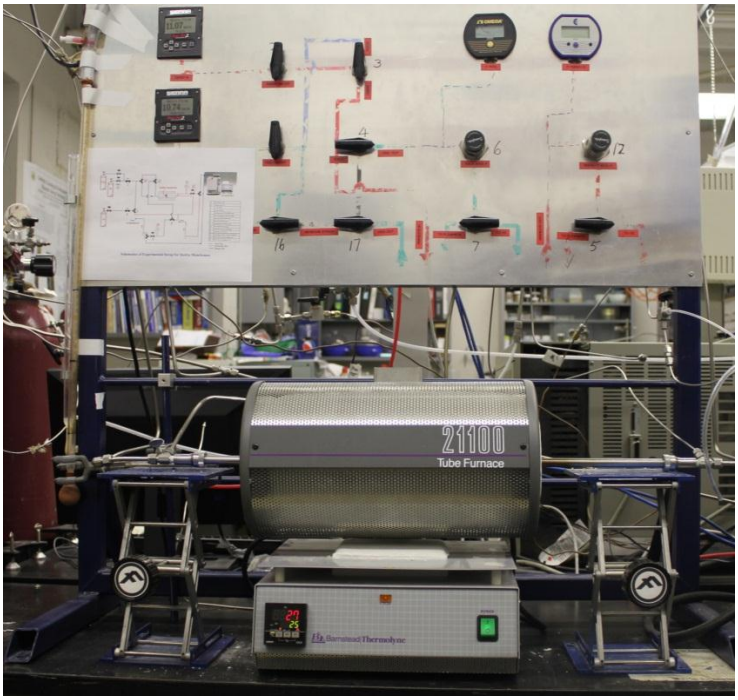

Figure 3.6 Permeation test set-up with the control panel with mass flow meters and pressure gages.

3.2. Material characterization

Material characterization is a crucial step before utilization of a chemical for a specific application. Knowing the characteristics of the investigated material will help us predict its potential uses as well as its limitations. Three characterization and two behaviour analysis were conducted for selected natural zeolites. These were aimed to understand the nature of the minerals/composites in terms of atomic level quality and macroscopic behaviour. XRD was used for phase identification and purity measurements. Scanning electron microscopy, Energy Dispersive X-ray and Inductively Coupled Plasma Mass Spectrometry were used for chemical composition analysis. High temperature treatment test and acid wash treatment were the tests to examine the stability of the selected natural zeolites.

3.2.1. X-ray diffraction (XRD)

XRD is one of the common techniques in crystallography. It is used to identify crystalline phases present in the sample. In this work phase identification for different samples was a proof of zeolite presence in the deposit under investigation. Characteristic zeolite peaks were indication of purity used for comparison between various samples. Using wavelengths in range of angstrom enables the beam to easily penetrate into a solid sample. The radiation is scattered by atoms in the lattice structures, thus using Bragg equation (3.7) the lattice spacing can be derived.

$$n\lambda = 2d\,\mathrm{Sin}(\theta) \quad n=1,2\ldots \tag{3.7}$$

Where d is the distance between two lattice planes, λ is X ray wavelength and θ is the angle between incoming X rays normal to the reflecting lattice plane. The integer n is called reflection order. In a Bragg-Brentano goniometer, there must be a stationary X-ray source,

usually Co or Cu, and a movable detector that scans the diffracted radiation intensities as a function of angle 2θ between the incoming and diffracted beams. The obtained patterns are then compared to databases usually available internationally (Warren, 1990).

Phase identification of precursor zeolite materials and prepared zeolite-cement matrix membranes were characterized by X-ray diffraction (Rigaku Geigerflex Power Diffractometer, Co tube, graphite monochromator). Minerals were tested as finely powdered as well as composite membranes (as were prepared explained in part 3.1.3)

3.2.2. Scanning electron microscopy–Energy dispersive x-ray spectroscopy (SEM-EDX)

Scanning electron microscopy is a versatile instrument for the study of microstructure of solid objects. SEM investigation was used in this study for morphology investigation. It was critical to observe the physical quality of zeolite and matrix interface with an SEM image as well as EDX analysis of the atomic contents of the region under investigation. Using a high energy beam of electrons SEM is capable of taking high resolution images on the order of 1-5 nm. A large depth of field in this scanning method makes it useful for morphology studies which require three dimensional appearance of the specimen.

Scanning electron microscope can also be used to obtain compositional information using energy dispersive x-ray spectroscopy (EDX). By measuring the scattered X-ray beams from the surface, a local atomic composition can be achieved (Goldstein, 2003).

For raw and composite zeolite Membranes surface morphology and surface composition were examined by SEM with energy dispersive x-ray spectroscopy (JEOL 6301F) .

3.2.3. Inductively Coupled Plasma Mass Spectrometry (ICP-MS)

ICP-MS is an analytical technique used to measure elemental composition. It consists of a time-varying magnetic field as an ion source and mass spectrometer as the ion separating and analysis agent (Becker, 2007). Atomic content can affect both framework structure and thermal behavior of natural zeolites. Therefore ICP-MS measurements were conducted to accurately measure each element content in a natural zeolite sample. Mordenite and clinoptilolite were analyzed with a Perkin Elmer Elan6000 quadrupole ICP-MS located in radiogenic isotope facility (RIF) at University of Alberta. Using a standard Na_2O_2 digesting method (Longerich, Jenner, Fryer, & Jackson, 1990) chemical elements of rocks/minerals can be detected.

3.2.4. High temperature stability test

As discussed in chapter two zeolite characteristics are attributed to its crystalline framework. Therefore it is crucial to measure the extent to which a zeolite sample can stand high temperatures without a change in its crystal structure. To examine the ability of natural zeolite to survive high temperature conditions, phase transformation were analyzed using XRD techniques after subjecting natural zeolite samples to a series of elevated temperatures. 16 samples, 1gram each, of clinoptilolite and mordenite, as received, were left in a muffle furnace with ramping temperature rate of 1 ^{o}C per minute. At 200,300,400…, 900 ^{o}C crucibles were taken out one by one. After cooling in desiccator all 16 samples were sent for X-ray phase identification. The same X-ray facility as described in Part 3.2.1 was used.

3.2.5. Acidic environment performance

Natural zeolite membrane application can be extended to liquid phase separation. Dealing with liquids with lower pH is very common to happen. To examine the acidic resistance of

natural zeolite, they were subjected to five different hydrochloric acid concentrations i.e. 1, 0.5, 0.1, 0.05, 0.01 M, as well as deionised water as a control. One gram of clinoptilolite sample was vigorously shaken in a 10 millilitre glass vial for 30 seconds, set aside for three different contact times and then liquid phase was sent to atomic absorption to measure the leached out cations.

Chapter 4: Results and analysis

4.1. Material Characterization results

This chapter is devoted to experimental and characterization results. In the first sections, atomic constituents of natural zeolite samples and X-ray patterns are shown. Both attribute to microscopic characteristics of zeolite. SEM analysis results are shown as the reflection of macroscopic quality of the embedding process. Thermal and acidic behaviour performances of the working material are shown in the last sections of characterization results. Gas permeation results are in the next section in this chapter.

4.1.1. X-ray diffraction (XRD)

X-ray diffraction results of three different clinoptilolite deposits are shown in Figure 4.1. All of the samples have strong characterization diffraction peaks of clinoptilolite crystals indicating the presence of clinoptilolite crystals; however sample number two has a minor peak indicating the presence of impurity. Figure 4.2 shows XRD comparison between mordenite and clinoptilolite used in this study. As discussed in Chapter 3 mordenite has a 12 member ring structure while clinoptilolite is a ten and eight member ring crystal. The XRD pattern comparison reflects the differences in unit cell symmetry. XRD patterns of raw zeolite powder and matrix membrane are shown in Figure 4.3. The XRD patterns for raw zeolite and matrix membrane show similarities except for some new peaks in the matrix sample. The similarity of the XRD patterns indicates that the clinoptilolite embedded in the Portland cement matrix after steam induced hydration reaction still preserves its crystalline structure. The new peaks that appeared at $2\theta=34.5^{o}$ and around 40^{o} in the matrix membrane were related to the cement

hydration products, C-S-H [6] and are an indication of the cement hydration occurrence (Grutzeck, Kwan, & DiCola, 2004; Janotka, 2003). In the samples with more cement we observed calcite formation which may be attributed to the presence of atmospheric carbon dioxide and highly reactive agents in the Portland cement.

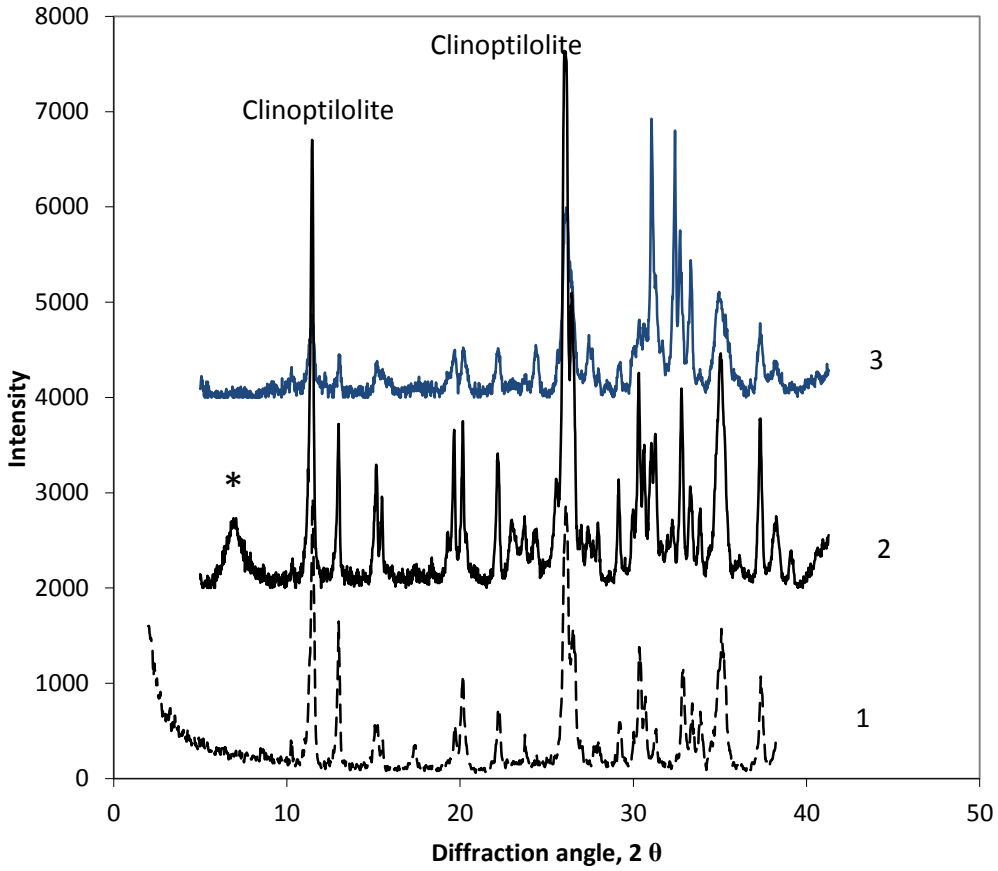

Figure 4.1 XRD pattern for clinoptilolite from three different deposits
* :impurity

[6] $CaO\text{-}SiO_2\text{-}H_2O$

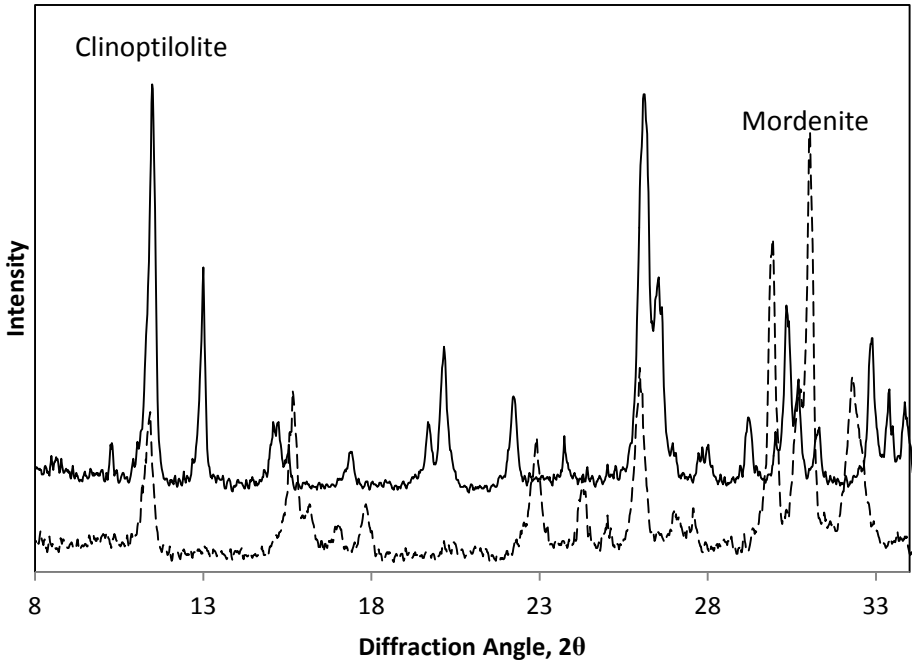

Figure 4.2 XRD pattern for clinoptilolite and mordenite powder

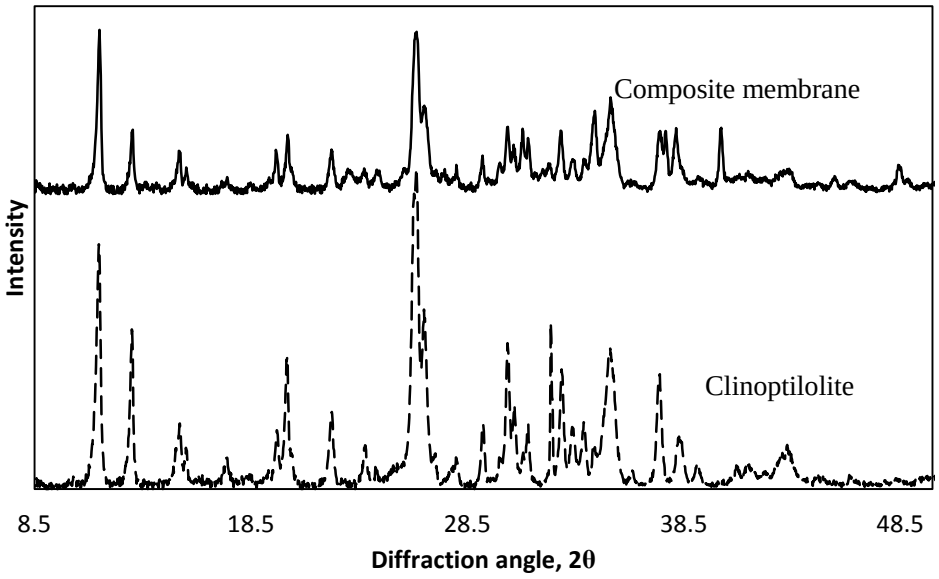

Figure 4.3 XRD pattern for clinoptilolite and composite zeolite membrane

4.1.2. Inductively Coupled Plasma Mass Spectrometry (ICP-MS)

Elemental mass percentage of clinoptilolite and mordenite were determined by ICP-MS. The results can be seen in Table 4.1 As expected aluminum content in clinoptilolite is less than mordenite by approximately 40%. Judging by the cation content it can be concluded that the clinoptilolite sample was predominantly sodium exchanged while the mordenite one was calcium rich in its pore framework.

Table 4.1 ICP-MS results

Analyte	**Na**	**Mg**	**Al**	**K**	**Ca**	**Fe**
Detection Limits (DL)	0.0019	0.1131	0.0003	0.0185	0.5511	0.0747
Clinoptilolite	19.68	1.29	47.50	23.79	4.12	3.62
Mordenite	7.63	1.45	33.82	3.49	44.53	9.08

4.1.3. Scanning electron microscopy–Energy dispersive x-ray spectroscopy (SEM-EDX)

High temperature steam cured cement is composed of dense intergrown networked crystals. These crystalline hydration products were expected to fill the gaps or crack defects in the composite structure (Lehmann, 2009) This physical bonding would act as the matrix holding zeolite particles in the membrane. SEM images of surface and cross-section of the cement matrix membrane are shown in Figure 4.4 and 4.5. The corresponding EDX analyses of the selected points are shown in Figure 4.6 a, b and c. Higher Ca content at point 2 from EDX analysis (the surroundings around the zeolite crystal) is an indication of a successful embedding of zeolite particle in the homogeneous dense cementitious matrix.

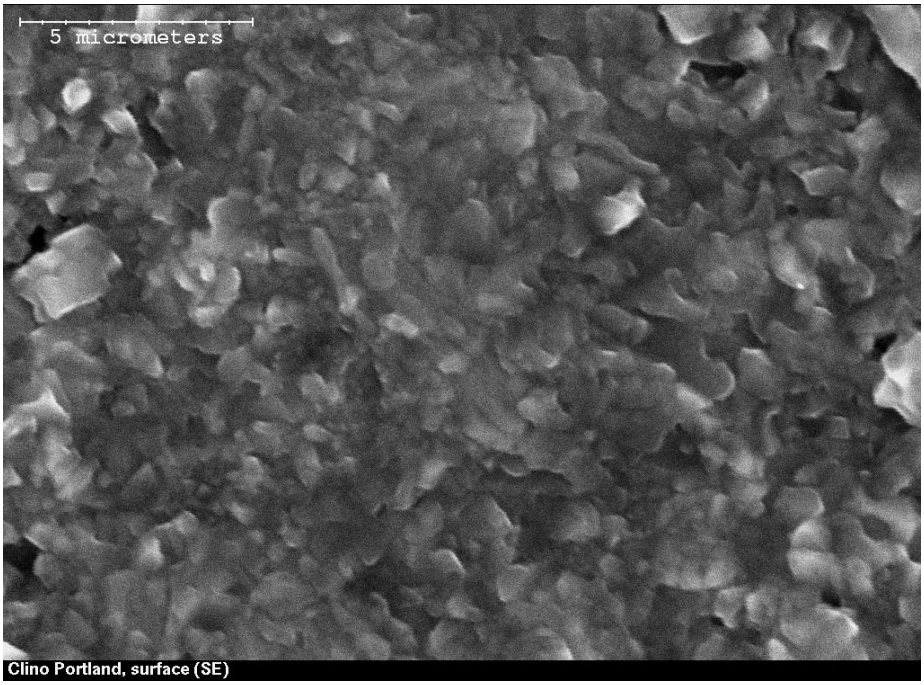

Figure 4.4 SEM image of clinoptilolite-composite membrane surface

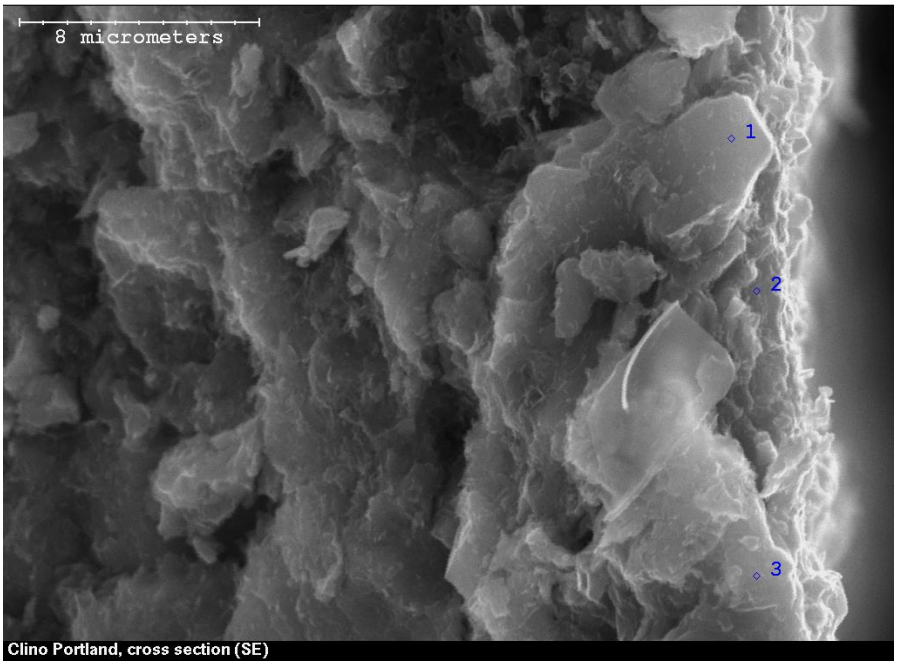

Figure 4.5 SEM image of the membrane cross-section with the points for EDX analysis

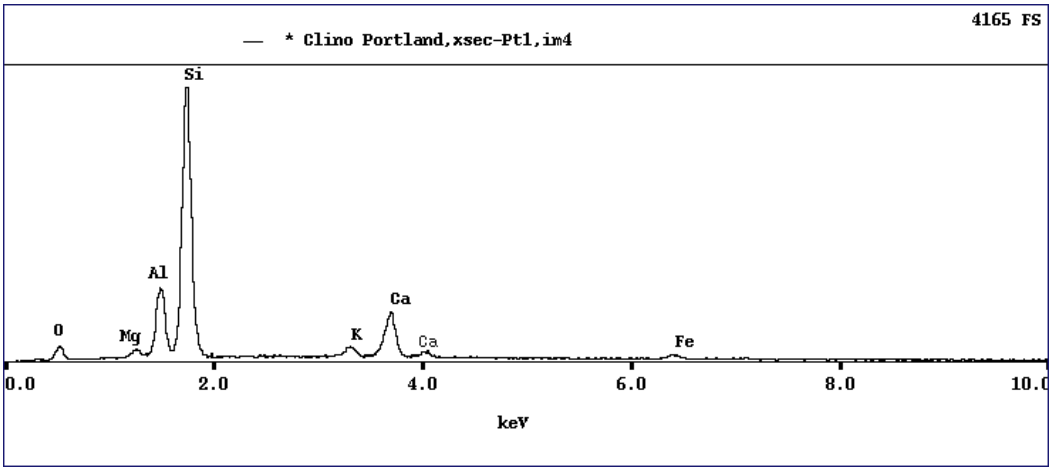

a

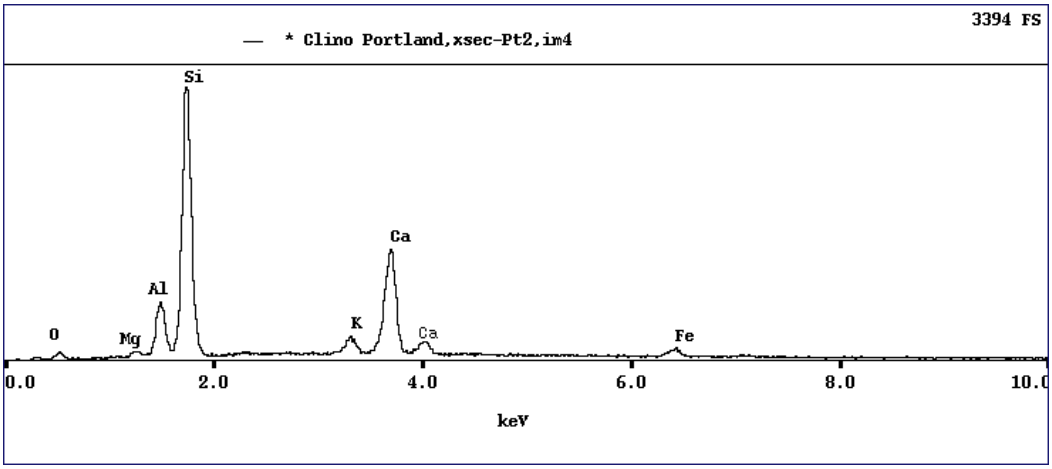

b

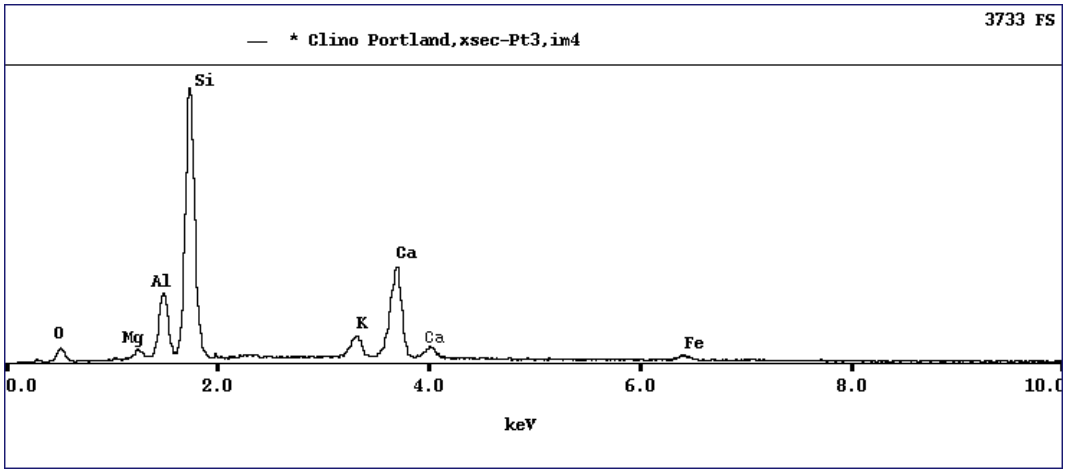

c

Figure 4.6 (a),(b),(c) EDX analysis of point 1, point 2, point 3, indicated in SEM image

4.1.4. High temperature stability performance

XRD patterns of clinoptilolite and mordenite samples after high temperature treatments are plotted in Figure 4.7 and 4.8. Crystalline structure of clinoptilolite samples are well retained up to temperatures around 700~800^{o}C. At 900 ^{o}C no crystalline phase in the clinoptilolite sample is detectable; however mordenite crystals are more stable than clinoptilolites and some degree of crystalline still can be observed even at temperature up to 900^{o}C.

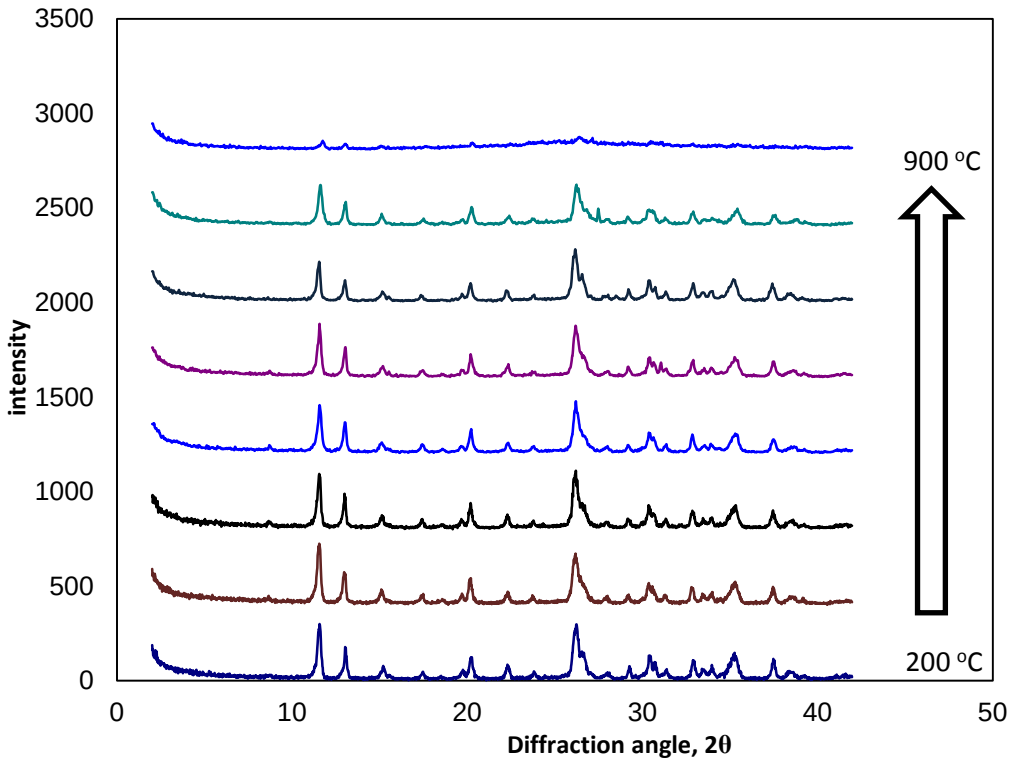

Figure 4.7 XRD pattern for clinoptilolite powder samples subjected to different temperatures

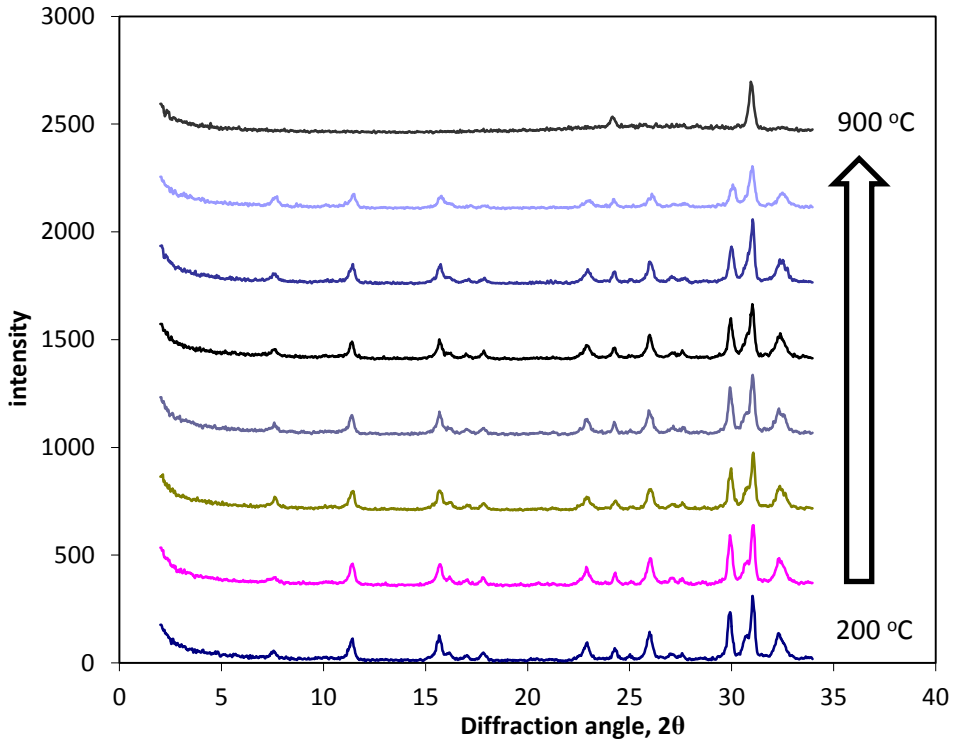

Figure 4.8 XRD pattern for mordenite powder samples subjected to different temperatures

4.1.5. Acidic environment performance

The amount of calcium leached out from the clinoptilolite sample into distilled water is compared to the value for 0.01M HCl in Figure 4.9. As expected, by increasing contact time, calcium concentration increases.

Acid environment is able to dissolve aluminum content of zeolite in Figures 4.10 and 4.11 aluminum concentration in the acid solution contacted with zeolite is presented in ppm units. Effect of contact time and acid molarity is as expected. It is worth to mention that 0.01M acid (corresponding to pH≈2) did not dissolve aluminum detectable by the instrument (1 ppm).

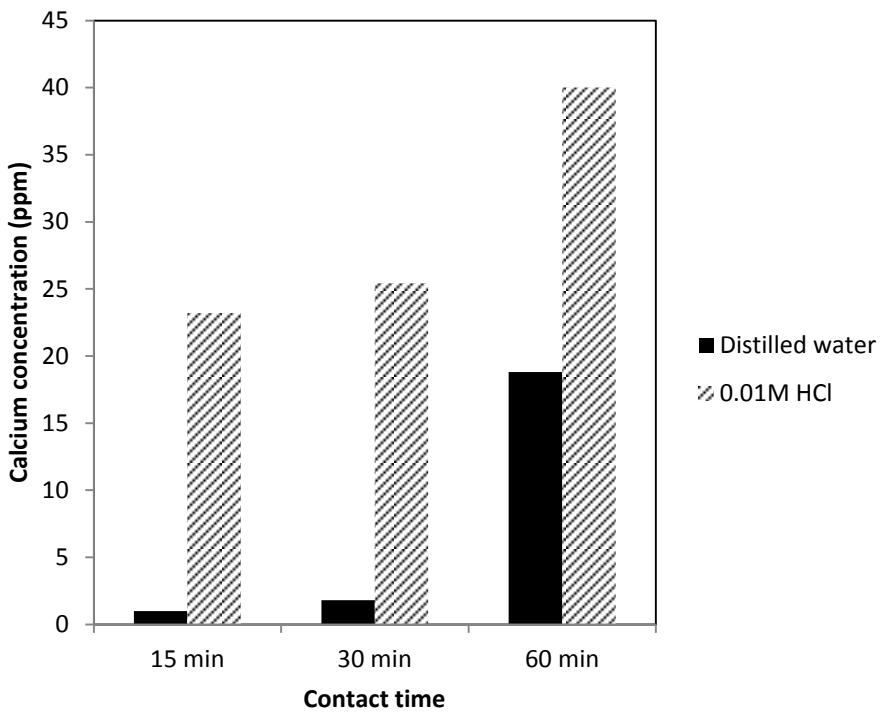

Figure 4.9 Calcium concentration, leached out of zeolite, clinoptilolite, in distilled water and 0.01M HCl, T=ambient, ±1 ppm

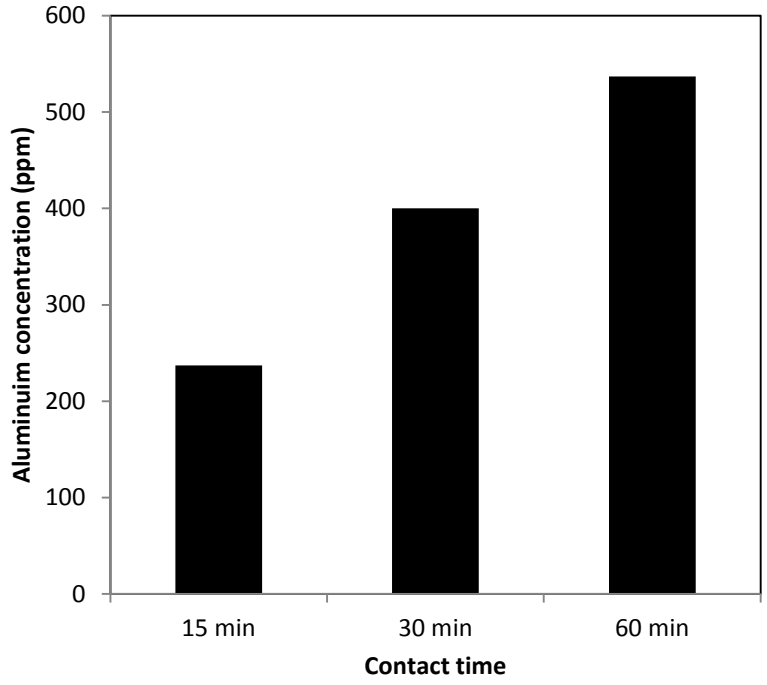

Figure 4.10 Aluminum concentration, leached out of zeolite, clinoptilolite, 1M HCl, T=ambient, ±1 ppm

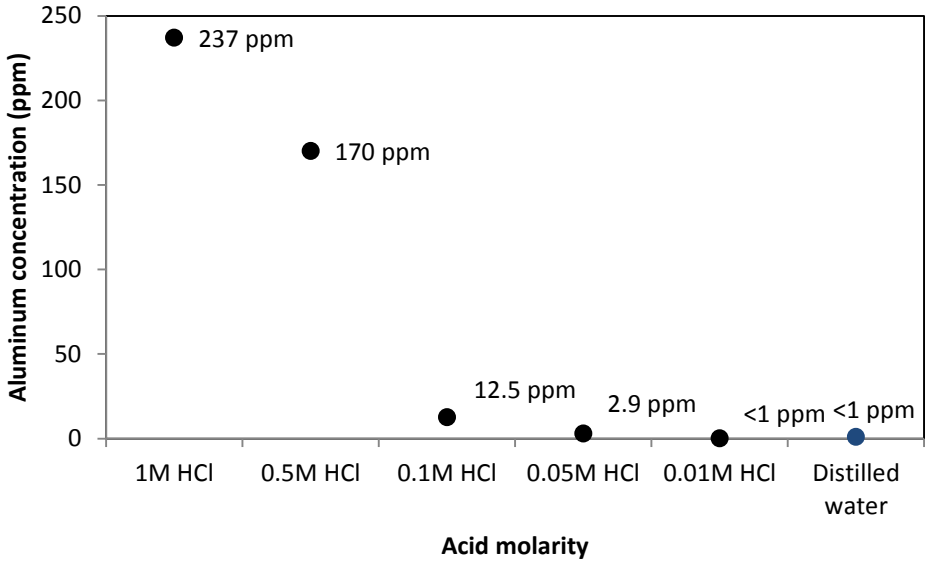

Figure 4.11 Aluminum concentration, leached out of zeolite, clinoptilolite, in different acid molarity, contact time= 15 minutes, T=ambient, ±1 ppm

4.2.Single Gas permeation test

A series of single gas permeation tests were performed on raw and composite membranes in order to:

a) Find the appropriate methodology for membrane preparation.

b) Investigate the permeation trend regarding temperature and transmembrane pressure in order to assess potential transport mechanism

c) Calculate the ideal selectivity of the membranes

4.2.1. Raw membrane performance

A control permeation test was performed with an alumina membrane and the results are plotted in Figure 4.12 and Figure 4.13. These tests were conducted to check the reliability of experimental set-up. The standard membrane performed classical Knudsen-range behaviour, i.e. an increasing permeation trend with transmembrane pressure difference and a slightly decreasing trend with permeation temperature.

Raw membranes were pre-treated and mounted in the experimental set up (Chapter 3). Permeation results for raw clinoptilolite and mordenite membranes are shown in Figure 4.14 and Figure 4.15 respectively. Ideal selectivity is calculated using equation 4.1

$$\alpha = \frac{Hydrogen\ permeance}{Carbon\ dioxide\ permeance} \quad (4.1)$$

For both natural zeolite samples raw membrane had an ideal selectivity above Knudsen predicted value diffusion (4.74 for H_2/CO_2) (Freeman, 2010). However limitation in manufacturability and scale-up necessitate introducing a procedure to improve membrane scale up as well as avoiding raw membrane drawbacks.

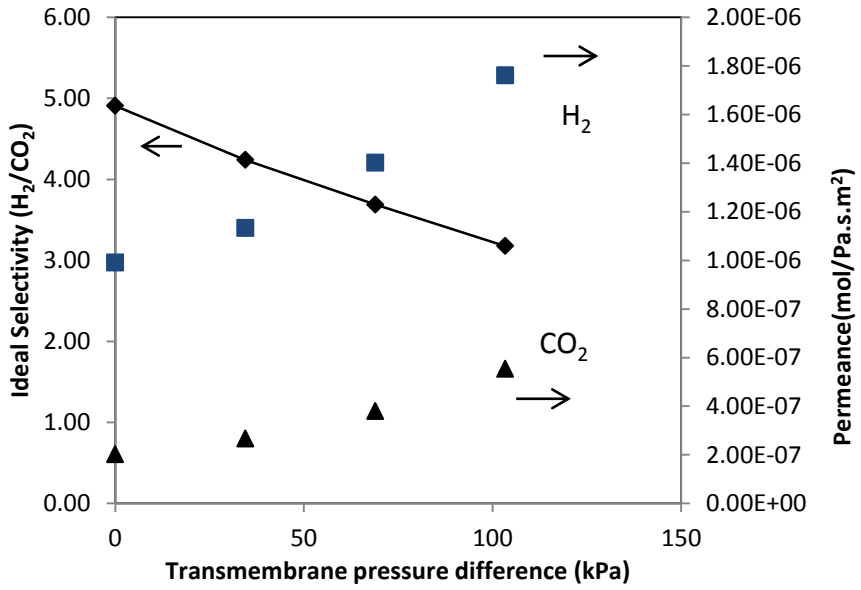

Figure 4.12 H_2 / CO_2 permeance and ideal selectivity for standard alumina membrane provided by GE, performed at room temperature.

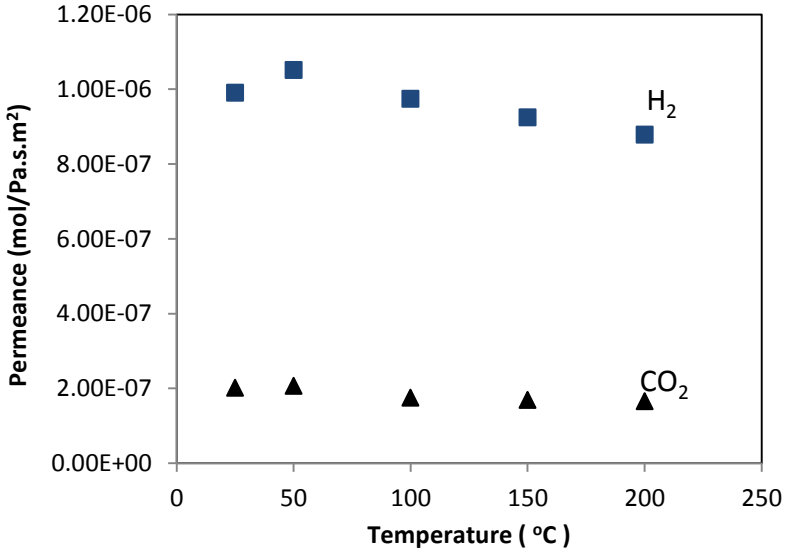

Figure 4.13 H_2 / CO_2 Permeance for standard alumina membrane provided by GE, ΔP=0 kPa.

Both hydrogen and carbon dioxide permeances were temperature dependent within the temperature range tested (Figures 4.14 and 4.15) and both gas permeances increased with increasing temperature. The temperature dependence of the gas permeance is an indication that the permeation through the zeolite-cement composite membranes is an activated diffusion process. The ideal selectivity of H_2 over CO_2 through the zeolite cement matrix membrane was higher than that predicted by Knudsen diffusion (4.74 for H_2/CO_2) (An et al., 2011).

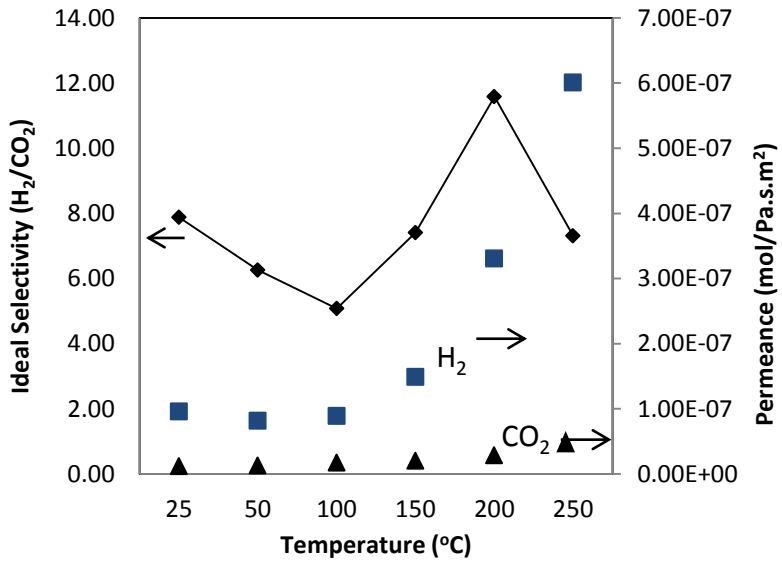

Figure 4.14 H_2 / CO_2 Permeance and ideal selectivity for raw clinoptilolite membrane pre-treated at 300 ^oC for 8 hours before permeation test, , ΔP=0 kPa.

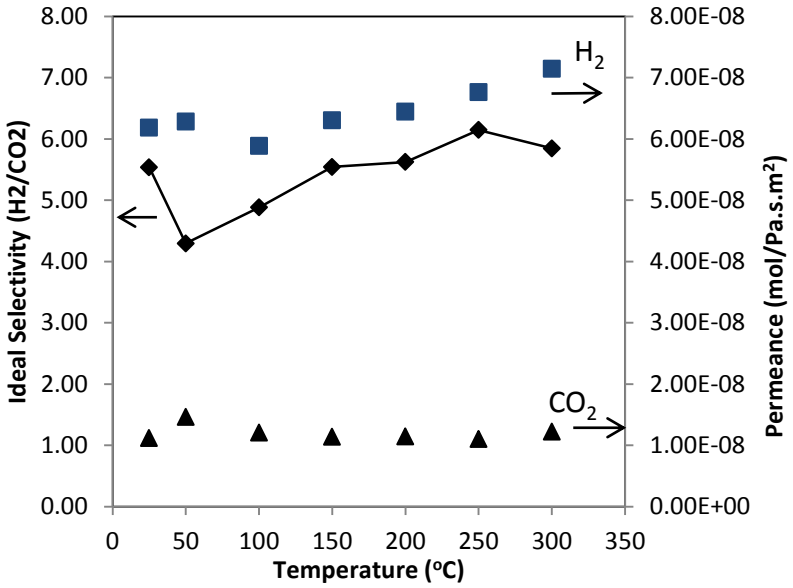

Figure 4.15 H_2 / CO_2 Permeance and ideal selectivity for raw mordenite membrane pre-treated at 300 ^{o}C for 8 hours before permeation test, , ΔP=0 kPa.

4.2.2. Composite membrane performance

Single gas permeation results (H_2 and CO_2) and their ideal selectivity over composite membranes with clinoptilolite/cement weight ratio of 75:25 are shown in Figure 4.16. This value was optimized by physical strength regarding zeolite content for clinoptilolite. Detailed value of all permeances and selectivities are presented in Appendix 1.

In general the accepted gas permeance mechanism for a gas molecule with a size close to that of the pore/channel of the zeolite (~ 3 Angstrom) is adsorption on the surface of the pore/channel, diffusion through the pore/channel and desorption from the surface of the opposite side of the membrane (Ackley & Rege, 2003). At a lower temperature (25^{o}C), higher selectivity of hydrogen over CO_2 can be attributed to the much stronger adsorption of CO_2 than hydrogen on the surface of the zeolite pore which restricts the diffusion of CO_2. At higher temperatures CO_2 adsorption on the surface of the zeolite pore is weakened and the mobility/diffusion of CO_2 is increased, resulting in lower H_2/CO_2 selectivity.

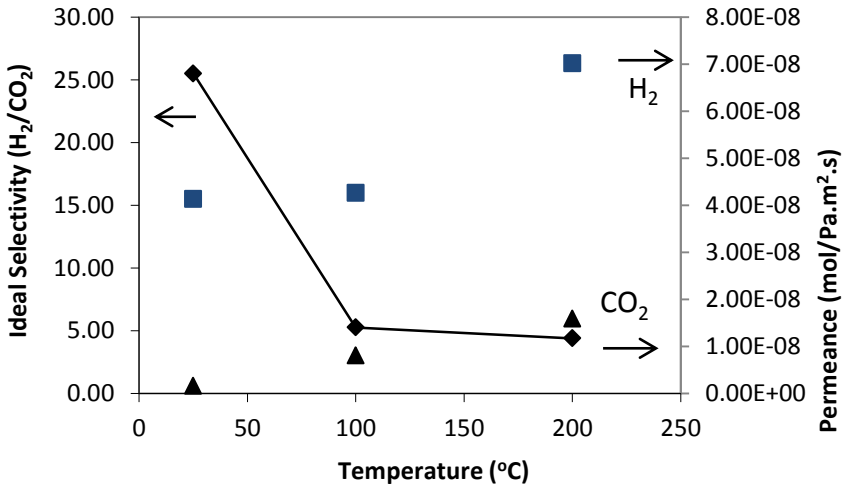

Figure 4.16 H_2 / CO_2 Permeance and ideal selectivity for composite clinoptilolite membrane pre-treated at 300 ^{o}C for 8 hours before permeation test, ΔP=0 kPa

Permeance and ideal selectivity for composite mordenite membrane pre-treated at 650°C are shown in Figure 4.17, while the effect of pre-treatment temperature on selectivity is shown in Figure 4.18 . Pre-treatment is shown to affect both permeation and selectivity. In the mordenite case an increase in selectivity was observed at higher pre-treatment temperatures. It may be explained by possible phase transformation of non-zeolite particles to a denser material. Melting of this small portion of surface crystals may have led to more zeolitic pore become available for gas separation.

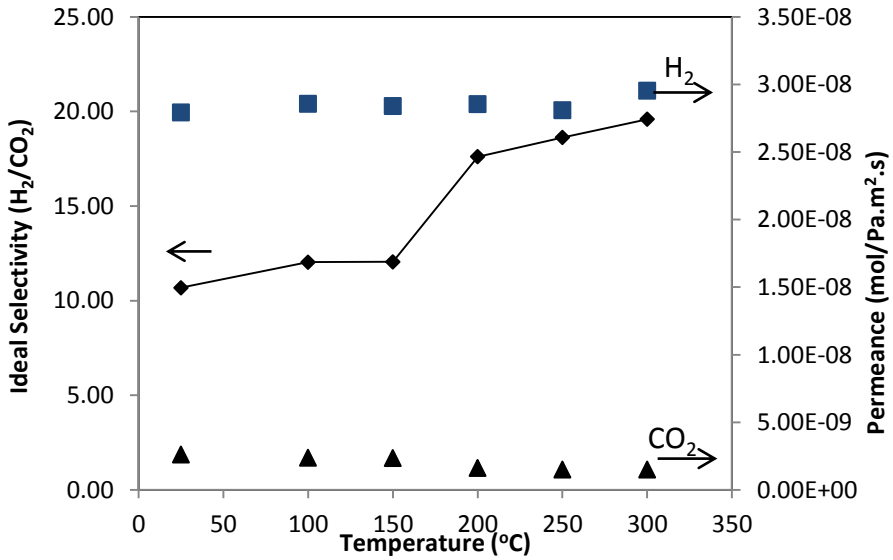

Figure 4.17 H_2 / CO_2 Permeance and ideal selectivity for composite mordenite membrane pre-treated at 650 °C for 8 hours before permeation test, ΔP=0 kPa.

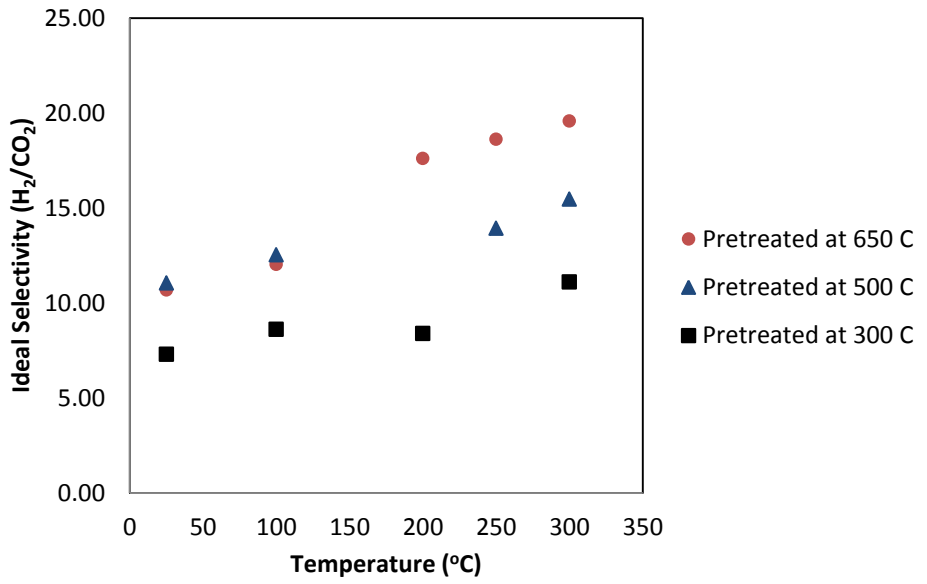

Figure 4.18 Ideal selectivity for mordenite-cement composite membrane pre-treated at 300, 500 and 650 ^{o}C for 8 hours before permeation test, ΔP=0 kPa.

Figure 4.19 and Table 4.2 show a comparison between a raw mordenite membrane and a composite mordenite-cement membrane pre-treated at the same temperature before the permeation test (350 ^{o}C). Results show that permeation is sacrificed for selectivity which could be the result of intercrystalline blockage by cement hydration products.

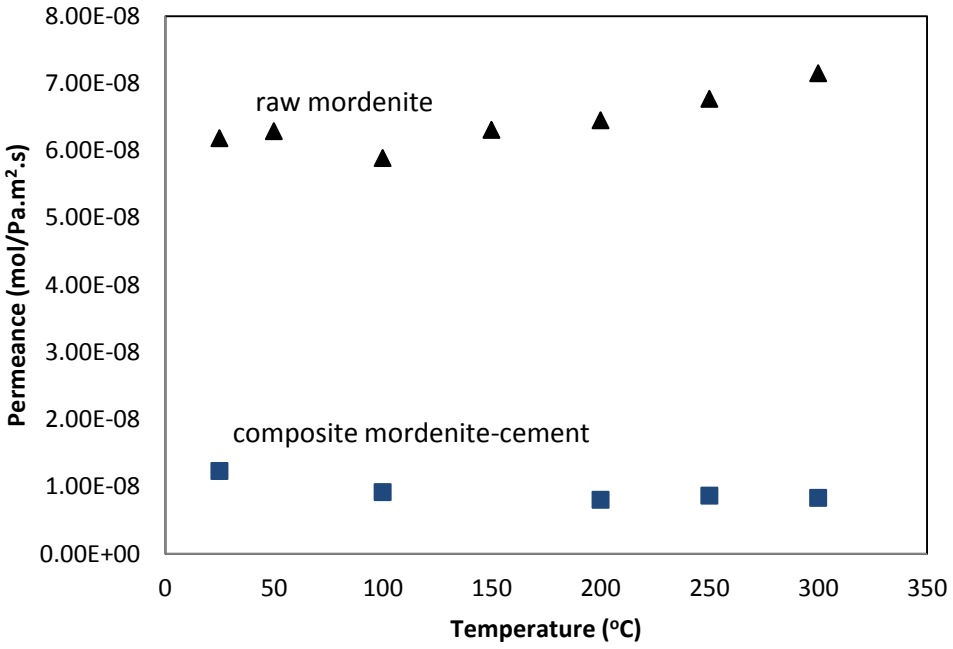

Figure 4.19 Hydrogen Permeance for raw versus composite mordenite membrane pre-treated at 350 ^{o}C for 8 hours before permeation test, ΔP=0 kPa.

Table 4.2 Selectivity for raw mordenite vs. mordenite-cement membrane pre-treated at 300^{o}C

Temperature (^{o}C)	raw mordenite	Composite mordenite-cement
25	5.54	7.29
100	4.88	8.62
200	5.62	8.40
300	5.85	11.11

Chapter 5: Summary and future work

5.1. Summary

(1) Novel approach to one of the most under-utilized mineral resources was experimentally examined. Raw natural zeolites, as mined, showed promising separation characteristics.

(2) A low-cost processable matrix material with good interface bonding between the separating agent (zeolite crystals) and matrix material was chosen.

(3) Thermal stability of zeolite was examined. Material behavior in a low pH environment was studied paving the path for potential liquid phase separation.

(4) A temperature dependent permeation trend was observed, which indicates activated diffusion mechanism. This phenomenon results in selective transportation through zeolite pores.

(5) XRD characterizations of the zeolite cement matrix membrane have demonstrated the occurrence of cement hydration under the high temperature steaming condition while zeolite content is still preserved.

(6) SEM analysis proved presence of intergrown cement hydration products with zeolite particles.

This study demonstrates a new low-cost approach to H_2 selective zeolite membranes for hydrogen separation at high temperature where chemical and physical stability are desired. Development of such zeolite/cement composites may result in the development of practical, robust H_2 separation membranes showing strong molecular sieving behavior under industrially relevant conditions.

5.2. Suggestions for future work

As most of industrial application of hydrogen selective membranes will involve high temperature steam, the effect of steam on crystal structure and permeation needs to be investigated. Modeling gas molecules transportation through natural zeolite membranes might shed more light on the nature of the zeolitic separation experimentally tested in this study. More separation areas are being tested by Dr. Kuznicki's research team, including water desalination and waste water treatment using natural zeolite membranes.

References

Ackley, M. W., & Rege, S. U. (2003). Application of natural zeolites in the purification and separation of gases. *Microporous and Mesoporous Materials, 61*(1-3), 25-42. doi: 10.1016/s1387-1811(03)00353-6

Adamiec, P., Benezet, J. C., & Benhassaine, A. (2008). Pozzolanic reactivity of silico-aluminous fly ash. *Particuology, 6*(2), 93-98. doi: 10.1016/j.partic.2007.09.003

Adhikari, S., & Fernando, S. (2006). Hydrogen Membrane Separation Techniques. *Industrial & Engineering Chemistry Research, 45*(3), 875-881. doi: 10.1021/ie050644l

Aguado, J. (2009). Catalytic cracking of polyethylene over zeolite mordenite with enhanced textural properties. *Journal of Analytical and Applied Pyrolysis, 85*(1-2), 352-358. doi: 10.1016/j.jaap.2008.10.009

Ahmadi, B., & Shekarchi, M. (2010). Use of natural zeolite as a supplementary cementitious material. *Cement & Concrete Composites, 32*(2), 134-141. doi: 10.1016/j.cemconcomp.2009.10.006

An, W. Z., Swenson, P., Wu, L., Waller, T., Ku, A., & Kuznicki, S. M. (2011). Selective separation of hydrogen from C(1)/C(2) hydrocarbons and CO(2) through dense natural zeolite membranes. *Journal of Membrane Science, 369*(1-2), 414-419. doi: 10.1016/j.memsci.2010.12.025

Apel, P. (2001). Track etching technique in membrane technology. *Radiation Measurements, 34*(1-6), 559-566. doi: 10.1016/s1350-4487(01)00228-1

Baker, R. W. (2007). *Membrane technology and applications*. Chichester Wiley.

Barbaa, D., Giacobbe, F., De Cesaris, A., Farace, A., Iaquaniellob, G., & Pipino, A. (2008). Membrane reforming in converting natural gas to hydrogen (part one). *International Journal of Hydrogen Energy*, *33*(14), 3700-3709. doi: 10.1016/j.ijhydene.2008.04.038

Becker, J. S. (2007). *Inorganic mass spectrometry : principles and applications*. Chichester, West Sussex, England: John Wiley & Sons.

Bekkum, H. ., Flanigen, E. M., Jansen, J. C., & Summer School on Zeolites. (1991). *Introduction to zeolite science and practice*. Amsterdam: Elsevier. Bird, R. B., Stewart, W. E., & Lightfoot, E. N. (1976). *Transport phenomena*. New York Wiley.

Bonneviot, L., & Kaliaguine, S. (1995). Zeolites a refined tool for designing catalytic sites : proceedings of the International Zeolite Symposium, Québec, Canada, October 15-20, 1995

Breck, D. W. (1973). *Zeolite molecular sieves : structure, chemistry, and use*. New York: Wiley.

Bye, G. C. (1999). *Portland cement : composition, production and properties*. London: Thomas Telford.

Cardew, P. T., Le, M. S., & Royal Society of Chemistry (Great Britain). (1998). *Membrane processes: A technology guide*. Cambridge: Royal Society of Chemistry

Caro, J., & Noack, M. (2008). Zeolite membranes - Recent developments and progress. *Microporous and Mesoporous Materials*, *115*(3), 215-233. doi: 10.1016/j.micromeso.2008.03.008

Caro, J., Noack, M., Kölsch, P., & Schäfer, R. (2000). Zeolite membranes - state of their development and perspective. *Microporous and Mesoporous Materials, 38*(1), 3-24. doi: 10.1016/s1387-1811(99)00295-4

Daoud, W. Z., & Renken, K. J. (2001). Laboratory assessment of flexible thin-film membranes as a passive barrier to radon gas diffusion. *Science of the Total Environment, 272*(1-3), 127-135. doi: 10.1016/s0048-9697(01)00676-3

Davis, M. E., & Lobo, R. F. (1992). Zeolite and Molecular-sieve Synthesis. *Chemistry of Materials, 4*(4), 756-768. doi: 10.1021/cm00022a005

Erdem, E., Karapinar, N., & Donat, R. (2004). The removal of heavy metal cations by natural zeolites. *Journal of Colloid and Interface Science, 280*(2), 309-314. doi: 10.1016/j.jcis.2004.08.028

Freeman, B. D., ÏAmpol′skiĭ, I. U. P., & International Congress on Membranes and Membrane Processes. (2010). *Membrane gas separation*. Chichester, West Sussex, U.K: John Wiley & Sons.

Frizon, E., & Galle, C. (2009). Experimental Investigations of Diffusive and Convective Transport of Inert Gas through Cement Pastes. *Journal of Porous Media, 12*(3), 221-237.

Goldstein, J. (2003). *Scanning electron microscopy and x-ray microanalysis*. New York: Kluwer Academic/Plenum Publishers.

Grutzeck, M., Kwan, S., & DiCola, M. (2004). Zeolite formation in alkali-activated cementitious systems. *Cement and Concrete Research, 34*(6), 949-955. doi: 10.1016/j.cemconres.2003.11.003

Guisnet, M., & Gilson, J.-P. (2002). *Zeolites for cleaner technologies*. London: Imperial college press.

Hafez, M. (1978). Fixation mechanism between zeolite and some radioactive elements. *Journal of Radioanalytical and Nuclear Chemistry, 47*(1), 115-119. doi: 10.1007/bf02517161

Hay, R. L. (1986). Geologic Occurrence of Zeolites and Some Associted Minerals. *Pure and Applied Chemistry, 58*(10), 1339-1342. doi: 10.1351/pac198658101339

Hewlett, P. (2008). *Lea's chemistry of cement and concrete*. Oxford: Elsevier Butterworth-Heinemann.

Janotka, I. (2003). Properties and utilization of zeolite-blended portland cements. *Clays and Clay Minerals, 51*(6), 616-624. doi: 10.1346/ccmn.2003.0510606

Jia, M. D., Chen, B. S., Noble, R. D., & Falconer, J. L. (1994). Ceramic-zeolite Composite Membranes and Their Application For Separation of Vapor Gas-Mixtures. *Journal of Membrane Science, 90*(1-2), 1-10. doi: 10.1016/0376-7388(94)80029-4

Junaid, A. S. M., Yin, H., Koenig, A., Swenson, P., Chowdhury, J., Burland, G., Kuznicki, S. M. (2009). Natural zeolite catalyzed cracking-assisted light hydrocarbon extraction of bitumen from Athabasca oilsands. *Applied Catalysis a-General, 354*(1-2), 44-49. doi: 10.1016/j.apcata.2008.11.006

Korkuna, O., Leboda, R., Skubiszewska-Zie¸ba, J., Vrublevs'ka, T., Gun'ko, V. M., & Ryczkowski, J. (2006). Structural and physicochemical properties of natural zeolites: clinoptilolite and mordenite. *Microporous and Mesoporous Materials, 87*(3), 243-254. doi: 10.1016/j.micromeso.2005.08.002

Kothari, R., Buddhi, D., & Sawhney, R. L. (2008). Comparison of environmental and economic aspects of various hydrogen production methods. *Renewable & Sustainable Energy Reviews, 12*(2), 553-563. doi: 10.1016/j.rser.2006.07.012

Kuznicki, S. M., McCaffrey, W. C., Bian, J., Wangen, E., Koenig, A., & Lin, C. C. H. (2007). Natural zeolite bitumen cracking and upgrading. *Microporous and Mesoporous Materials, 105*(3), 268-272. doi: 10.1016/j.micromeso.2007.03.034

Lawson, K. W., & Lloyd, D. R. (1997). Membrane distillation. *Journal of Membrane Science, 124*(1), 1-25. doi: 10.1016/s0376-7388(96)00236-0

Lee, K. P., Arnot, T. C., & Mattia, D. (2011). A review of reverse osmosis membrane materials for desalination-Development to date and future potential. *Journal of Membrane Science, 370*(1-2), 1-22. doi: 10.1016/j.memsci.2010.12.036

Lehmann, C. (2009). *Evolution of Phases and Micro Structure in Hydrothermally Cured Ultra-High Performance Concrete (UHPC).* Nanotechnology in Construction 3 2009, Part 3, 287-293, DOI: 10.1007/978-3-642-00980-8_38

Li, X., Zhou, C., Lin, Z., Rocha, J., Lito, P. F., Santiago, A. S., & Silva, C. M. (2011). Titanosilicate AM-3 membrane: A new potential candidate for H2 separation.

Microporous and Mesoporous Materials, *137*(1-3), 43-48. doi: 10.1016/j.micromeso.2010.08.019

Longerich, H. P., Jenner, G. A., Fryer, B. J., & Jackson, S. E. (1990). Inductively coupled plasma-mass spectrometric analysis of geological samples: A critical evaluation based on case studies. *Chemical Geology, 83*(1-2), 105-118. doi: 10.1016/0009-2541(90)90143-u

McCusker, L. B., Olson, D., & Baerlocher, C. (2007). *Atlas of zeolites structures*. Amsterdam: Elsevier.

Mendes, A. M., Magalhaes, F. D., & Costa, C. A. V. (2006). *New trends on membrane science* (Vol. 219). Dordrecht: Springer.

Miller, S. J., Koros, W. J., & Vu, D. Q. (2007). Mixed matrix membrane technology: enhancing gas separations with polymer/molecular sieve composites. In Z. G. J. C. Ruren Xu & Y. Wenfu (Eds.), *Studies in Surface Science and Catalysis* (Vol. Volume 170, pp. 1590-1596): Elsevier.

Mizutani, Y., Nakamura, S., Kaneko, S., & Okamura, K. (1993). Microporous Polyoropylene Seets. *Industrial & Engineering Chemistry Research, 32*(1), 221-227. doi: 10.1021/ie00013a029

Nenoff, T. M., Spontak, R. J., & Aberg, C. M. (2006). Membranes for hydrogen purification: An important step toward a hydrogen-based economy. *Mrs Bulletin, 31*(10), 735-741. doi: 10.1557/mrs2006.186

Ok, Y. S. (2007). Heavy metal adsorption by a formulated zeolite-Portland cement mixture. *Journal of Hazardous Materials, 147*(1-2), 91-96. doi: 10.1016/j.jhazmat.2006.12.046

Ortega, E. A., Cheeseman, C., Knight, J., & Loizidou, M. (2000). Properties of alkali-activated clinoptilolite. *Cement and Concrete Research, 30*(10), 1641-1646. doi: 10.1016/s0008-8846(00)00331-8

Paixão, V. (2010). Modification of MOR by desilication treatments: Structural, textural and acidic characterization. *Microporous and Mesoporous Materials, 131*(1-3), 350-357. doi: 10.1016/j.micromeso.2010.01.013

Park, J.-H., & Sudarshan, T. S. (2001). *Chemical vapor deposition*. Materials Park, OH: ASM International.

Perraki, T., Kakali, G., & Kontoleon, F. (2003). The effect of natural zeolites on the early hydration of Portland cement. *Microporous and Mesoporous Materials, 61*(1-3), 205-212. doi: 10.1016/s1387-1811(03)00369-x

Robeson, L. M. (1999). Polymer membranes for gas separation. *Current Opinion in Solid State & Materials Science, 4*(6), 549-552. doi: 10.1016/s1359-0286(00)00014-0

Robson, H. E. (2001). *Verified syntheses of zeolitic materials*. Amsterdam: Elsevier.

Sadeghi, F., Ajji, A., & Carreau, P. J. (2007). Analysis of microporous membranes obtained from polypropylene films by stretching. *Journal of Membrane Science, 292*(1-2), 62-71. doi: 10.1016/j.memsci.2007.01.023

Sand, L. B. (1978). *Natural Zeolites : Occurence, Properties, Use*. Oxford: Pergamon Press.

Sebastian, V., Lin, Z., Rocha, J., Tellez, C., Santamaria, J., & Coronas, J. (2006). Synthesis, Characterization, and Separation Properties of Sn— and Ti—Silicate Umbite Membranes. *ChemInform, 37*(30), no-no. doi: 10.1002/chin.200630218

Seidel, A. (2007). *Kirk-Othmer encyclopedia of chemical technology. Index to volumes 1-26*. Hoboken (N. J.): Wiley-Interscience.

Süer, M. G., Baç, N., & Yilmaz, L. (1994). Gas permeation characteristics of polymer-zeolite mixed matrix membranes. *Journal of Membrane Science, 91*(1-2), 77-86. doi: 10.1016/0376-7388(94)00018-2

Taylor, H. F. W. (1990). *Cement chemistry*. London; San Diego: Academic Press.

Warren, B. E. (1990). *X-ray diffraction*. New York: Dover Publications.

Wienk, I. M., Boom, R. M., Beerlage, M. A. M., Bulte, A. M. W., Smolders, C. A., & Strathmann, H. (1996). Recent advances in the formation of phase inversion membranes made from amorphous or semi-crystalline polymers. *Journal of Membrane Science, 113*(2), 361-371. doi: 10.1016/0376-7388(95)00256-1

Zeolites and catalysis Vol. 1. (2010). Weinheim: Wiley-VCH-Verl.

Zimmerman, C. M., Singh, A., & Koros, W. J. (1997). Tailoring mixed matrix composite membranes for gas separations. *Journal of Membrane Science, 137*(1-2), 145-154. doi: 10.1016/s0376-7388(97)00194-4

Appendix 1

Detailed list of runs along with their standard deviation are presented here. In error calculation formula (A.1) was used.

Standard deviation based on the entire population (STDEV.P) = $\sqrt{\frac{(x-\bar{x})^2}{n}}$

Where x is the sample mean average (number1, number2, …) and n is the sample size.

Each Experiment was run for at least three times and reproducibility runs where conducted with making three membranes for each membrane set.

GEMEM-YSZ Standard membrane 1, H_2, Permeation		
Temperature (^oC)		STDEVP
25	9.91E-07	1.9656E-08
50	1.05E-06	2.72396E-09
100	9.74E-07	7.36261E-09
150	9.25E-07	3.68465E-09
200	8.79E-07	3.96235E-09
300	8.61E-07	1.15092E-08

GEMEM-YSZ Standard membrane 1, CO_2, Permeation		
Temperature (^oC)		STDEVP
25	2.02E-07	3.47957E-09
50	2.06E-07	7.33761E-09
100	1.75E-07	4.31555E-10
150	1.69E-07	8.31476E-09
200	1.66E-07	9.03654E-10
300	2.02E-07	3.47957E-09

RAW clinoptilolite, pre-treated at 300 ^oC, H_2, Permeation		
Temperature (^oC)		STDEVP
25	1.22E-08	6.43248E-09
50	1.31E-08	5.13375E-09
100	1.75E-08	2.12945E-09
150	2.01E-08	1.06133E-09
200	2.85E-08	2.99447E-08
250	8.22E-08	1.00198E-07
300	2.12E-07	7.28921E-07

RAW clinoptilolite, pre-treated at 300 ^oC, CO_2, Permeation		
Temperature (^oC)		STDEVP
25	9.60E-08	3.18403E-09
50	8.19E-08	4.58203E-10
100	8.90E-08	1.73289E-10
150	1.49E-07	3.61877E-09
200	3.31E-07	6.39074E-09
250	6.01E-07	1.54837E-08
300	1.97E-06	3.10383E-08

RAW mordenite, pre-treated at 650 °C, H_2, Permeation		
Temperature (°C)		STDEVP
25	6.18E-08	1.49959E-09
50	6.29E-08	7.81703E-10
100	5.89E-08	1.27091E-09
150	6.31E-08	7.13722E-10
200	6.45E-08	4.44153E-10
250	6.77E-08	1.30172E-09
300	7.15E-08	3.13093E-09

RAW mordenite, pre-treated at 650 °C, CO_2, Permeation		
Temperature (°C)		STDEVP
25	1.12E-08	3.1E-09
50	1.46E-08	1.8E-09
100	1.21E-08	6.9E-11
150	1.14E-08	0
200	1.15E-08	5.2E-10
250	1.10E-08	6.4E-11
300	1.22E-08	5.7E-10

Composite clinoptilolite-cement membrane, pre-treated at 300 °C, H_2, Permeation		
Temperature (°C)		STDEVP
25	4.13E-08	2.3E-09
100	4.26E-08	7E-11
200	7.01E-08	5.1E-09

Composite clinoptilolite-cement membrane, pre-treated at 300 °C, CO_2, Permeation		
Temperature (°C)		STDEVP
25	1.62E-09	6.5E-11
100	8.09E-09	1.7E-10
200	1.59E-08	4.2E-09

Composite mordenite-cement membrane, pre-treated at 650 °C, H_2, Permeation		
Temperature (°C)		STDEVP
25	2.79E-08	9.7E-10
100	2.86E-08	8.1E-10
150	2.84E-08	1.6E-10
200	2.85E-08	2.7E-10
250	2.81E-08	5.8E-10
300	2.95E-08	8.2E-10

Composite mordenite-cement membrane, pre-treated at 650 °C, CO_2, Permeation		
Temperature (°C)		STDEVP
25	2.61E-09	7.1E-11
100	2.37E-09	3.1E-10
150	2.36E-09	1.9E-10
200	1.62E-09	1.3E-10
250	1.51E-09	0
300	1.51E-09	0

Composite mordenite-cement membrane, pre-treated at 300 ^{o}C, H_2, Permeation		
Temperature (^{o}C)		STDEVP
25	9.60E-08	3.18403E-09
100	8.19E-08	4.58203E-10
150	8.90E-08	1.73289E-10
200	1.49E-07	3.61877E-09
250	3.31E-07	6.39074E-09
300	6.01E-07	1.54837E-08

Composite mordenite-cement membrane, pre-treated at 300 ^{o}C, CO_2, Permeation		
Temperature (^{o}C)		STDEVP
25	1.22E-08	6.43248E-09
100	1.31E-08	5.13375E-09
150	1.75E-08	2.12945E-09
200	2.01E-08	1.06133E-09
250	2.85E-08	2.99447E-08
300	8.22E-08	1.00198E-07

Composite mordenite-cement membrane, pre-treated at 500 ^{o}C, H_2, Permeation		
Temperature (^{o}C)		STDEVP
25	2.50E-08	8.08E-10
100	2.91E-08	7.2757E-10
200	4.64E-08	1.0532E-09
250	4.90E-08	5.6729E-10
300	5.29E-08	1.6216E-10